
Institute of Biomechanics
Stremayrgasse 16-II
8010 Graz, Austria

# Master Thesis

## Viscoelastic and poroelastic properties of porcine and human brain tissues

to achieve the degree of
Master of Science

**Author:** David Walk, BSc
**Supervisor:** Gerhard Sommer, PhD

**Head of Institute:** Professor Gerhard A. Holzapfel, PhD

September 4, 2017

# Contents

# Abstract - Englisch

The brain is one of the most important organs in our body and therefor any injuries applied to the head, such as traumatic brain injury or shaken baby syndrome, but also tumor growth or hydrocephalus lead to life-threatening or severe repercussions. Hence, many researches, over the course of the last several decades, conducted studies to describe the biomechanics of the brain. Although many studies were conducted to characterize the mechanics of the brain, it is far from being complete. The reason for that are the limited availability of human brain samples, the broad variation in tissue qualities and the fact that only a few studies exist, which describe the viscoelastic behavior of the human brain.

Therefore, this master thesis analyses the viscoelastic and poroelastic properties of porcine and human brain tissue based on a literature research and combined multiaxial shear tests under compression and tension. This experimental data will not only be used to characterize the mechanical properties of the brain but will further be used to perform computational simulations, which enable the prediction of the mechanical properties of the brain tissue in health and disease. With the aid of these simulations smart protection systems could be developed and it can also be used to predict brain development and disease progression.

# Abstract - German

Da das Gehirn eines der wichtigsten Organe in unserem Körper ist, können jegliche Einwirkungen auf den Kopf, sei es durch Schädel-Hirn-Trauma oder dem Schütteltrauma bei Säuglingen aber auch durch Tumorwachstum oder Hydrozephalus, zu lebensbedrohlichen oder schwerwiegenden Folgen führen. Daher beschäftigten sich viele Wissenschaftler mit der Beschreibung der biomechanischen Eigenschaften des Gehirns. Obwohl viele Studien durchgeführt wurden um die Mechanik des Gehirns zu charakterisieren, ist diese noch weit davon entfernt vollständig zu sein. Der Grund dafür sind die geringe Verfügbarkeit von Humanproben, die Unterschiede in der Qualität der Proben und die Tatsache, dass es nur wenige viskoelastische Studien am menschlichen Gehirn gibt.

Deshalb werden in dieser Masterarbeit, mit Hilfe einer Literaturrecherche und kombinierten multiaxialen Experimenten unter Druck und Zug, die viskoelastischen und poroelastischen Eigenschalften von Schwein- und Humanproben analysiert. Die Daten dieser Experimente werden nicht nur zur Charakterisierung der mechanischen Eigenschaften des Gehirns sonder auch zur computerunterstützten Simulation, welche die Vorhersage der mechanischen Eigenschaften des Gehirns in Gesundheit und Krankheit ermöglicht. Mit Hilfe dieser Simulationen ist es möglich intelligente Schutzsysteme zu entwickeln sowie die Entwicklung des Gehirns als auch den Fortschritt von Krankheiten vorherzusagen.

# Acknowledgment

First of all I would like to thank my supervisor Dr. Gerhard Sommer for his great support and guidance during my master thesis. He not only explained the experiments and the theory of biomechanics of the brain to me, but also provided me with good advice, whenever necessary. I also want to thank Prof. Haybäck and Töglhofer MSc from the neuropathology department for providing me with human brain samples.

I would also like to thank my brother Simon and my sister Hannah, for always providing me with literature and good advice during this thesis.

Last but not least I would like to thank my parents and my girlfriend for always supporting and encouraging me during this thesis but also during my whole study.

# 1 Introduction

The human brain is one of the most important organs in our body and therefore any injuries applied to the head could lead to life-threatening or severe repercussions. Hence, many researchers, over the course of the last several decades, were interested in the characterization of the mechanical properties of brain tissue [Bilston et al., 1997] [Van Dommelen et al., 2010]. Even though a great number of studies where conducted to describe the biomechanics of the brain [Miller and Chinzei, 1997] [Miller and Chinzei, 2002] [Rashid et al., 2013], only little is known about its mechanical properties, due to the broad variation in the tissues qualities, as described in Goriely et al. [2015]. The majority of these studies were conducted to prevent injuries such as traumatic brain injuries or diseases such as hydrocephalus or tumor growth [Bilston et al., 1997].

Considering all the functions of the brain it is obvious that any neurological and physical influence could lead to severe implications to our daily life and even our future. One of the main injuries and pathological changes of the brain are for example the traumatic brain injury or shaken baby syndrome, split brain syndrome, tumor growth or hydrocephalus.

Traumatic brain injury (TBI) is declared as a public health problem and it is still one of the major sources of deaths and disabilities world wide as described in Langlois et al. [2006a] and Greve and Zink [2009]. TBI often occurs due to mechanical impacts on the head, for example in virtue of traffic and sports accidents but also falls [Jennett, 1996]. According to literature 10 million cases of severe TBIs, resulting in death or hospitalization, occur annually [Langlois et al., 2006b]. Depending on the intensity and the type of mechanical impact, traumatic brain injuries could lead to cranial bruise, skull fracture, cerebral concussion, contusion and traumatic hematoma.

These brain injuries can be classified according to their severity, associated injuries or if they are covered or open [Mumenthaler and Mattle, 2006]. The cardinal symptom for traumatic brain injuries is unconsciousness, which might also lead to disturbances of memory. These symptoms could be accompanied by epileptic seizure or neurological malfunction [Mumenthaler and Mattle, 2006]. The depth of the coma resulting from a TBI can be rated by the Glasgow-Coma-Scale. Thereby the patient gets evaluated by its verbal response, motorical reactions and the movement of his eyes. Each response will be assessed with a number ranging from 3 to 15 points. 15 points indicate best performance and 3 points a severe one [Mumenthaler and Mattle, 2006] [Morris, 2010]. As described in Mumenthaler and Mattle [2006], traumatic brain injuries can be diagnosed with X-rays of the

skull or the cervical vertebra but also with a CT or MRI [Mumenthaler and Mattle, 2006]. Furthermore due to the fact that traumatic brain injuries occur due to a sudden impact on the brain, it is important to perform viscoelastic tests to be able to implement a viscoelastic model, that is able to simulate such injuries. In this thesis I try to tackle the problem of finding such models by performing and discussing experiments which provide further results on the viscoelastic properties of the brain tissue.

Another common disease is the so-called hydrocephalus. It is characterized by an increase of the liquor, due to a malfunctions of the drainage or insufficient resorption, which leads to an augmentation of the intracranial pressure, as described in Masuhr et al. [2013]. In other words it describes the extension of the inner and outer subarachnoid spaces [Mumenthaler and Mattle, 2006]. According to literature three types of hydrocephalus can be distinguished. The first one is the so-called occlusion hydrocephalus, including ventricular obstruction and occlusion of the foramina. The next one is the communing hydrocephalus, which describes perturbations of the liquor resorption and the last one is the hypersecretory hydrocephalus. It describes an overproduction of liquor without circulation disorders [Masuhr et al., 2013]. The symptoms of a hydrocephalus are for example abnormal head size or protrusion of the frontal bone [Mumenthaler and Mattle, 2006]. For a better understanding of the occurrence of this disease it is necessary to analyze the poroelastic properties of the brain tissue. With this test it might also be possible to prevent the appearance of such a disease. Therefore this thesis includes a literature research about the oedometric test, which is used to describe the poroelastic properties of the brain.

Under consideration of the above mentioned injuries and diseases it is obvious that computational simulations, which are used to predict the mechanical behavior of the human brain in health and disease are very important. With the aid of these simulations smart protections systems can be developed, which could prevent TBI, and it can also be used to predict brain development and disease progression, used for an earlier diagnose or even obstruction of hydrocephalus or brain tumor.

## 1.1 The Human Brain

The brain not only is the control center, which directly or indirectly controls our actions in daily life, but it also regulates other body parts, for example via the distribution of hormones [Kahle and Frotscher, 1991]. It is part of the central nervous system and consists of very soft biological tissue that is composed of three meninges. The outer meninx is the so-called dura mater also referred to as pachymeninx and the inner meninges are the leptomeninx [Ferner, 1973] [Kahle and Frotscher, 1991]. It consists of the arachniodea and the pia mater [Kahle and Frotscher, 1991].

The dura mater is a thick, tearproof, connective tissue mainly consisting of collagen fibers. It functions as a capsula fibrosa to mechanically stabilize the brain as described in Waldeyer [2009]. This meninx is closely attached to the inside of the cranium and at the same time forms the periost, which is a tissue layer, that surrounds the bones. The dura mater also forms the tentorium cerebelli, which separates the upper cranial cavity [Ferner, 1973] [Kahle and Frotscher, 1991] [Waldeyer, 2009].

Following the dura mater the next cerebral membrane is the arachnoid mater, which is attached to the inside of the dura mater [Kahle and Frotscher, 1991]. These two meninges are separated by a capillary gap, the so-called spatium subdurale. It embeds the liquor containing subarachnoid space, the cavum subarachnoideale [Kahle and Frotscher, 1991]. The exterior part of the arachnoidea is a non-vascular tissue, which is impermeable for liquor. Between the arachnoid and the innermost meninx, the pia mater, is the subarachnoid space, which is filled with the cerebrospinal fluid. These two maters are connected by connective tissue filaments, the trabeculae. These trabeculae are responsible for the name of this meninx, as they are arranged like radial spider webs across the arachnoidea mater [Ferner, 1973] [Kahle and Frotscher, 1991] [Waldeyer, 2009].

The third meninx, the pia mater, covers the whole structure of the brain, with all its whorls and sulci and it consists of thin connective tissue [Ferner, 1973]. It forms the pia-glia border and starting from the pia mater, vessels proceed to the brain substance, as described in Kahle and Frotscher [1991] Waldeyer [2009]. Within these meninges lies the brain.
It can be divided in four main regions. The cerebrum, the diencephalon, the cerebellum and the brain stem.

The cerebrum consists of the two hemispheres [Ferner, 1973], the so-called left and right hemisphere. Their surface is composed of sulci and gyri. These sulci can be further devided into the primary, secondary and tertiary sulci [Kahle and Frotscher, 1991]. The hemispheres consist of the subarachnoid space, also called lateral ventricles, the basal ganglia, which contains for example the nucleus caudatus and the putamen, and the pallium. The pallium consists of the white substance and the cerebral cortex [Ferner, 1973].

Each hemisphere is divided into four lobes, the lobus frontalis, the lobus parientalis, the lobus temporalis and the lobus occipitalis [Kahle and Frotscher, 1991].

The hemispheres are connected with each other by the corpus callosum and other small interconnections (commissura anterior, commissura fornicis) [Kahle and Frotscher, 1991] [Waldeyer, 2009]. The purpose of the corpus callosum is the exchange of information and the coordination of the two hemispheres. As described in Kahle and Frotscher [1991] the consciousness is bound to the cerebral cortex, therefore only the sensory inputs, which are transmitted to the cortex, will be consciously perceived. The left hemisphere obtains the information of the right body part and the right hemisphere the information of the left body part [Kahle and Frotscher, 1991] [Waldeyer, 2009].

The next region is the diencephalon. It consists of the epithalamus, the thalamus dorsalis, the subthalamus and the hypothalamus. The diencephalon not only transfers the sensorical and motorical signals to the cerebrum or controls physical and psychological events but it is also involved in the sleep-wake cycle [Kahle and Frotscher, 1991]. In addition to that it is responsible for the coordination of all the sensory input [Ferner, 1973] [Kahle and Frotscher, 1991].
The third region is the cerebellum. It is the integration center for the coordination and delicate adjustment of the body movement and for the regulation of the myotonus [Kahle and Frotscher, 1991]. According to literature the cerebellum is further responsible for the maintenance of the balance [Ferner, 1973]. It is a transverse positioned part of the brain with an approximate size of a goose egg [Ferner, 1973].

The last and fourth region is the brain stem. It is subdivided into three segments [Kahle and Frotscher, 1991]. The first segment is the medulla oblongata. It forms the junction from the spinal cord to the brain. The second region is the pons. It shapes a broad bulge, with distinct transverse fibers [Kahle and Frotscher, 1991]. The third region is the mesencephalon. The mesencephalon consists of the pedunculi cerebri. The brain stem is, for example, responsible for the interconnection and the processing of the sensory impression and the motorical information [Kahle and Frotscher, 1991].

## 1.2 Related Work

Over the course of the last decades many researchers were interested in the characterization of the mechanical properties of brain tissue [Hrapko et al., 2006, Prevost et al., 2011a, Weickenmeier et al., 2016]. This interest in the biomechanics of the human brain started shortly after the recognition that any neurological or physical damage to the brain could lead to severe repercussions to our daily life and even our future [de Rooij and Kuhl, 2016]. These studies were not only used to provide a better insight into the mechanical properties of the brain but also to develop realistic constitutive models for the brain [Tada et al., 1994, Hrapko et al., 2008b, Budday et al., 2017b,a].

Due to the limited availability of human brain samples, which were for example used in the studies of Medige [1997], Franceschini et al. [2006], Jin et al. [2013], Budday et al. [2017a], many researchers alternatively used animal brain samples. That is the reason why some studies were conducted with porcine samples [Miller and Chinzei, 1997, 2002, Rashid et al., 2013, Destrade et al., 2015] and bovine samples [Bilston et al., 1997, 2001, Darvish and Crandall, 2001, Cheng and Bilston, 2007, Laksari et al., 2012]. This was possible due to the structural similarity of porcine and bovine brain samples. Other studies tested the properties for example of rat brains [Gefen et al., 2003] [Elkin et al., 2010].

These studies have significantly contributed to the better understanding of the mechanical response of brain tissue. Inferring and drawing conclusions for the human brain from experiments conducted on different species might lead to false assumptions, as they are not identical to human brain tissue, as described in Margulies and Prange [2002]. Due to the small size of the porcine brain, some studies performed their tests with specimens that consist of a mixture of gray and white mater [Prevost et al., 2011b]. As a matter of fact these results could not be compared to human brain samples which only consist of either gray or white mater [Rashid et al., 2013]. As a consequence the size of the specimens in this thesis has been chosen to be so small that all samples only consisted of one mater with the intention to produce results from porcine samples, which are suitable for comparison with human brain samples, because this thesis also contains results from human brain samples.

Most of these studies only focused on one loading condition. Porcine and human samples have for example been tested in shear [Medige, 1997] [Margulies and Prange, 2002] [Hrapko et al., 2006] [Rashid et al., 2013] [Budday et al., 2017a], compression [Miller and Chinzei, 1997] [TAMURA et al., 2007] [Hrapko et al., 2008b] [Prevost et al., 2011a] [Laksari et al., 2012] and tension [Miller and Chinzei, 2002] [Tamura et al., 2008] [Rashid et al., 2014] [Labus and Puttlitz, 2016]. To the best of the authors knowledge only a few studies have applied multiple loading conditions, which are necessary for computational simulations, as it was the case in the studies of Margulies and Prange [2002], Hrapko et al. [2008b] and Jin et al. [2013].

The study of Jin et al. [2013] applied compression, tension and shear tests on human brain samples. In the study of Hrapko et al. [2008a] shear, compression and relaxation tests were applied on porcine brain specimens. The study of Margulies and Prange [2002] used shear and compression tests to describe the brain biomechanics, only the studies of Hrapko et al. [2008a], Budday et al. [2017a,b] applied experiments on the same specimen, to reduce the effect of inter-sample variation [Hrapko et al., 2008a].

Due to the fact that up to now only a few studies applied experiments on the same sample, this thesis was used to further characterize the mechanical properties of the brain, as the results of previous studies vary significantly, depending for example on the testing pro-

tocol, shape of the samples, testing method and environmental influences. Therefore the main purpose of this thesis was to describe the characterization of the brain tissue, as a combination of tension, compression and shear experiments were performed and all tests were applied on the same sample.

Such a combination of experiments has so far only been applied in the study of Budday et al. [2017b], therefore it is necessary to conduct more studies, which perform combined experiments.

# 2 Methods

## 2.1 Material

The porcine brains used in this thesis were acquired from the Merkur supermarket and the butchery Hutter and the human brain sample was acquired from the Medical University of Graz. A total of five porcine brain specimens were used. After harvesting these samples from the above mentioned locations, they were then directly transported to the laboratory, where the experiments took place. Due to the fact that the butcher has to examine the spinal cord for diseases before selling the meat, the porcine was cut along its sagittal plane. As a consequence, the cerebral hemispheres of all porcine brain specimens were separated and a correct allocation of the white matter was impossible most of the time. Figure 2.1 depicts the two hemisphere of a porcine brain.

Figure 2.1: Hemispheres of a porcine brain.

Due to the limited availability of human brain specimens, a total of one sample was acquired from the pathology department of the Medical University of Graz. From each brain a 1.5 cm thick coronal slice was received. It was important that this slice included the following four regions: corpus callosum, basal ganglia, corona radiata and the cortex.

These regions were used to describe the regional dependencies of the brain tissue. This slice was kept refrigerated at 3°C and humidified with phosphate-buffered saline solution (PBS) until testing. The human brain slice which has been used in this thesis can be seen in Fig. 2.2.

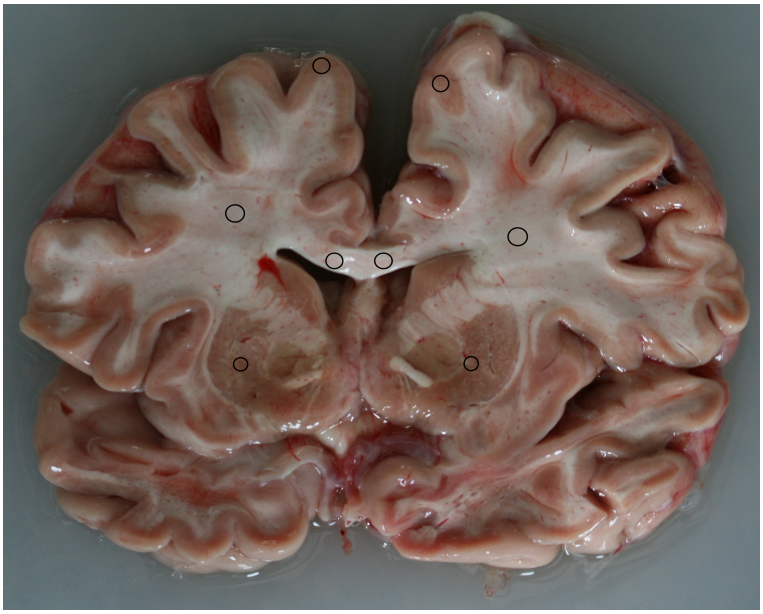

Figure 2.2: Coronal slice of the human brain.

## 2.2 Specimen Preparation

To reduce tissue degradation and alteration all brain samples were kept refrigerated at 3°C and humidified with 0.9% phosphate buffered saline solution, as described in Van Dommelen et al. [2010]. As the mechanical properties of the brain tissue would have changed if the samples would have been stored in the freezer, it was important to start the experiments as soon as possible after receiving them [Fallenstein et al., 1969]. Before the actual preparation of a specimen it was necessary that all used utensils and even the gloves were humidified with PBS, as otherwise the brain tissue would adhere to it and might be damaged as it detaches and as a consequence can't be used for the experiments. The consistency of the tissue could be compared to a soft gel. Therefore each specimen was refrigerated just before the preparation started, so that the tissue wouldn't loose its stiffness. This was a very useful trick to facilitate the preparation.

Afterwards the cooled tissue was taken from the fridge, to prepare cube shaped specimens with a side length of 5 mm from the above mentioned regions. The restriction of the cubes side length to 5 mm, was due to the limited thickness of the cortex. To prepare

a specimen suitable for this thesis a scalpel, tweezer and a ruler were used. Although all these precautions were met, the soft nature of the brain tissue caused a deformation of the specimen under their own weight during preparation and mounting [Budday et al., 2017a].

Not only the fiber direction played an important role while preparing the specimens, but also the composition of the cubes. To achieve significant results, it was important to ensure, that the cubes did only consist either of gray or white matter, since a mixture of these matters would result in inexplicable and incomparable mechanical results. As described in Kahle and Frotscher [1991] the substantia grisea is composed of neural cells and the substantia alba consists of a network of fibers, i.e. extensions of the neural cells, which appear to be bright due to their white coating. Figure 2.3a depicts a prepared cube from the basal ganglia, consisting of gray matter, while Figure 2.3b depicts the corona radiata, composed of white matter. As shown in Figs. 2.3a and 2.3b the specimens were glued to the upper specimen holder. Sandpaper was beforehand fixated on the holder, to ensure a better fixation of the specimen.

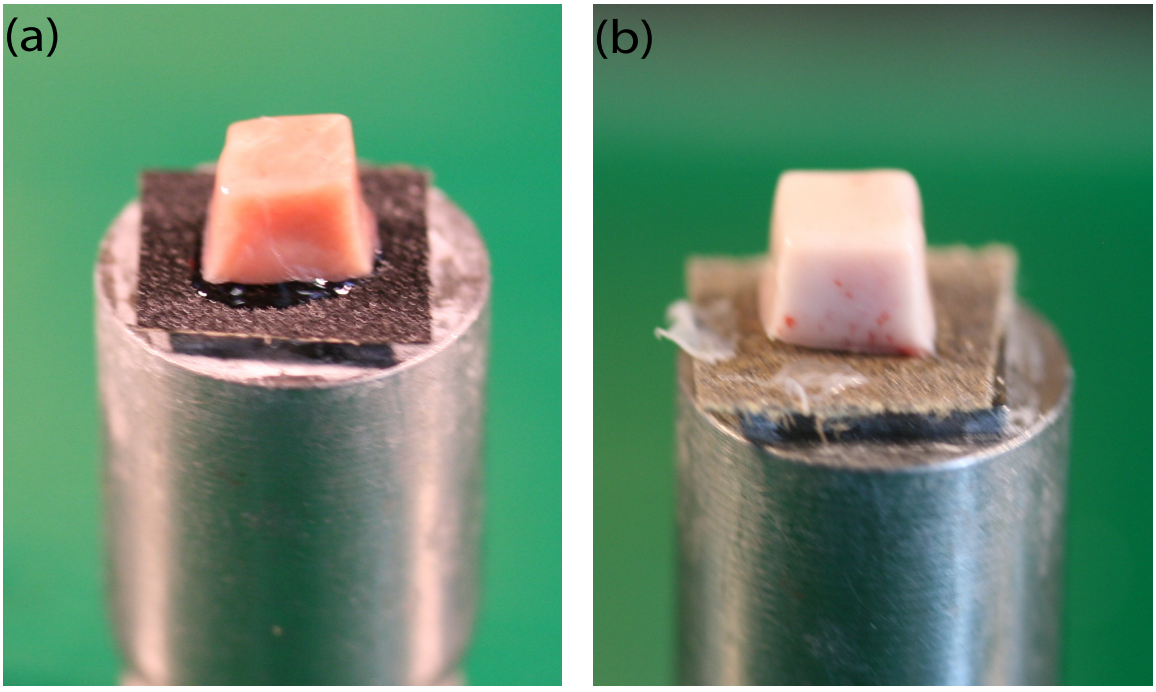


Figure 2.3: Representative cube shaped gray matter sample of the basal ganglia (a) and white matter sample from the corona radiata (b) with a 5 mm side length glued to the upper specimen holder

In Figs. 2.4 and 2.5 the prepared specimens of the cortex and the corpus callosum can be seen. Figures 2.3a and 2.4 the basal ganglia as well as the cortex consist of gray matter and the corona radiata and the corpus callosum of white matter.

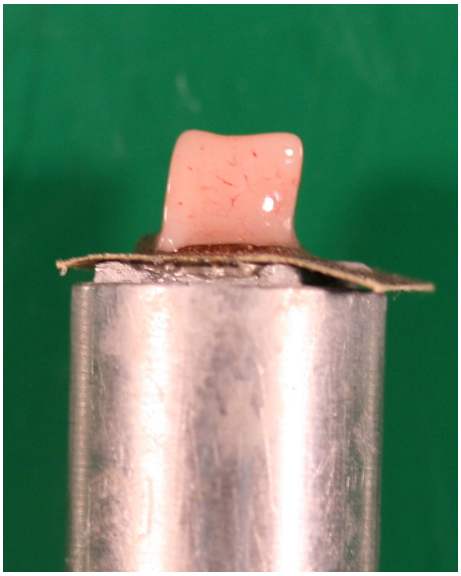

Figure 2.4: Representative sample of the cortex with a 5mm side length glued to the upper specimen holder.

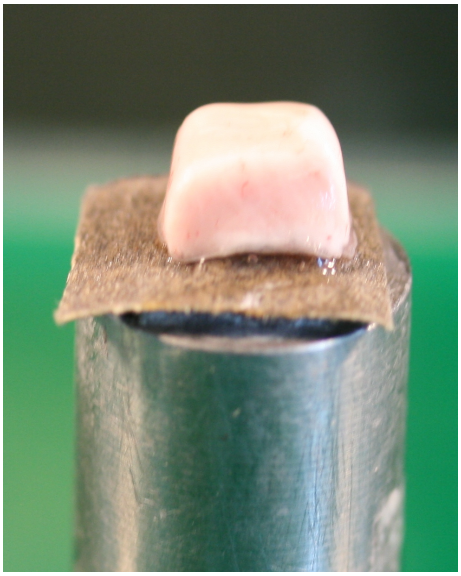

Figure 2.5: Representative sample of the corpus callosum with a 5mm side length glued to the upper specimen holder.

## 2.3 Experimental Setup

For the realization of the experiments a triaxial testing machine (Fig. 2.6) was used. After the correct extraction and preparation, each cube was glued on the upper specimen holder of the triaxial testing device. As mentioned in the previous section the sandpaper was used to ensure a better fixation of the specimen in the testing device. To prevent the tissue from slipping off the holder, the cube itself was first glued on the upper specimen holder with a super adhesive, which can also be seen for example in Fig. 2.3a. Before the experiment could start, the container of the testing device, which contained 0.9% PBS, was manually moved to the starting position. As the testing protocol, which will be described in section 2.4, lasts for about 2 hours and 15 minutes, it was necessary to perform all tests with a PBS filled container, as the specimen would be drained, due to the duration of the test.

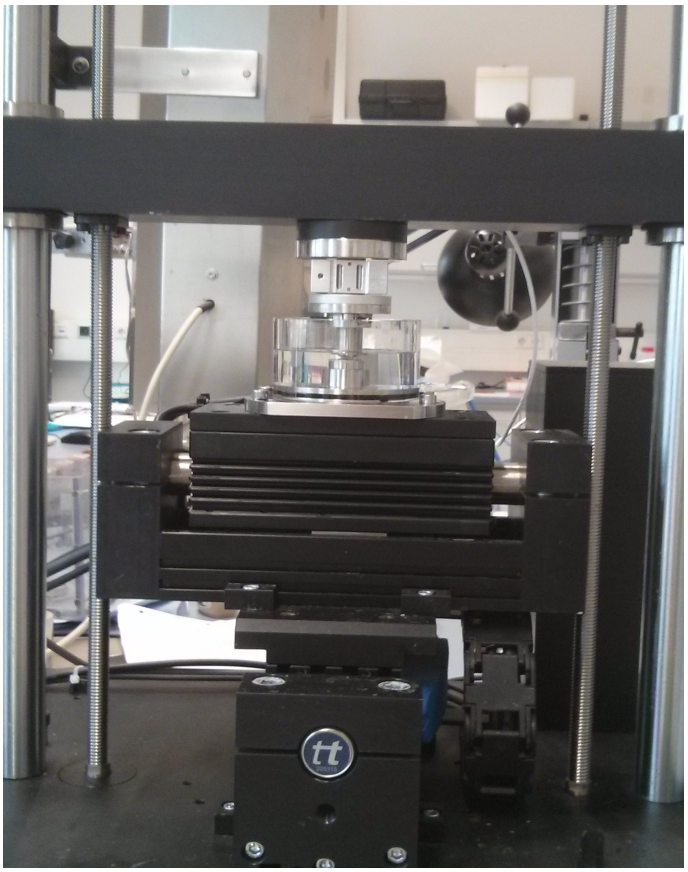

Figure 2.6: Experimental setup of the triaxial testing device. The upper part consists of the load cell which is attached to the upper specimen holder. The container is filled with PBS, which prevents dehydration of the specimen. The actuator in z-direction is located above the load cell. The other two actuators in x- and x-direction are located beneath the lower specimen holder.

At first a super adhesive was used to fixate the sample on the upper cylindrical specimen holder. Afterwards the upper and lower specimen holder were fixated in the testing device, then the forces were set to zero and the actual testing procedure was ready to start. At the beginning of the experiment the container moved directly under the upper specimen holder. Once these two parts were on top of each other the test has to be stopped and the super adhesive was applied on the lower cylindrical part. These two parts were then moved together until a preload of about 10mN was applied. This compression force has been held for 300 seconds, to ensure the hardening of the glue, which was very important as otherwise the specimen would slip from the testing device. After the expiration of the 300 seconds the testing protocol could start and the two holders moved apart until the preload was reduced to zero. Figure 2.7 depicts an exemplary brain sample tested in the triaxial testing machine.

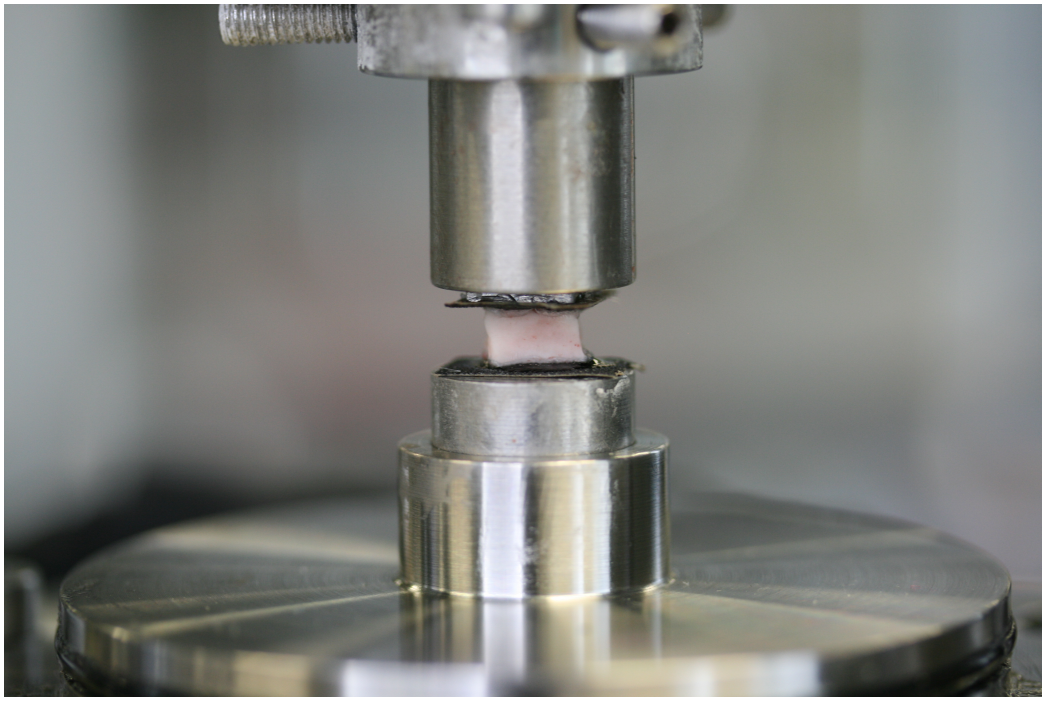

Figure 2.7: Tested brain sample of a porcine brain.

Afterwards the container was either filled with PBS or artificial cerebrospinal fluid (CSF) until the specimen was fully covered. This was important as it prevented the specimen from drainage. On the one hand it was important to have enough fluid in the container to cover the sample, but on the other hand not too much so that perturbations to the upper specimen holder could influence the results. One of the main problems while testing was to ensure that the specimen didn't detach from the device. Some tests have been conducted at room temperature and some at 37°C to experimentally determine, if there are any differences in the mechanical properties of the tissue under room temperature or 37°C.

## 2.4 Test Protocol

For all experiments presented in this thesis one testing protocol was used. This protocol consisted of a combination of tests: the simple shear test under compression, the shear relaxation test under compression, the simple shear test under tension and the shear relaxation test under tension. The sequence can be seen in Table 2.1. With the aid of a 10N class 1 strain gauge-load cell the force, which was applied during the tests, was measured.

Then, the testing sequence started with a simple shear test, followed by a shear relaxation test under no compression, both with an amount of shear of 0.2. For the shear tests a strain rate of 2 mm/min and for the shear relaxation test a strain rate of 100 mm/min was used. Then the specimen was compressed by 5% of its initial thickness and the same tests took place. After each trial, which consisted of a simple shear followed by a shear relaxation test, the compressive strain increased by 5% until a maximum of 25% was reached. Then the combined tension tests at 5% tension started. The tension rate also increased in 5% steps until an overall tension of 25% was reached and after that the testing protocol ended.

For the shear relaxation tests a rapid shear step was applied. This displacement was held for 300s and a normalized nominal stress vs. time response was plotted, which can be seen in Section 3.

Table 2.1: Sequence of the combined test protocol.

| | |
|---|---|
| 1 | Simple shear at 0% compression at an amount of shear of $\gamma = 0.2$<br>2 preconditioning and 1 main cycle |
| 2 | Shear relaxation at 0% compression at an amount of shear of $\gamma = 0.2$ |
| 3 | Compression of the specimen dependent on the initial sample thickness, with 5% compression steps until a final compression of 25% was reached. At each compression step simple shear was applied in analogous to step 1 and 2. |
| 4 | Simple shear at 5% tension at an amount of shear of $\gamma = 0.2$<br>2 preconditioning and 1 main cycle |
| 5 | Shear relaxation at 5% tension at an amount of shear of $\gamma = 0.2$ |
| 6 | Tension of the specimen dependent on the samples thickness, with 5% tension steps until an overall tension of 25% was reached. At each tension step simple shear was applied in analogous to step 1 and 2. |

For the simple shear tests a sinusoidal load was applied, which means that the speed

slowed down when it reached the turning points. First two preconditioning cycles took place and then the third main cycle was recorded.

## 2.5 Data Acquisition and Processing

For each experiment the testing time as well as the displacement and the stress were calculated and recorded. Additionally the thickness, the width of the specimen, the applied speed, the strain and the number of cycles were recorded in a tra-file for each sample. All plots, which can be seen in the results, were generated with the software MATLAB. For the reduction of noise a so-called Savitzky-Golay filter was applied. It is a digital filter used to smoothen the data to increase the signal-to-noise ratio without falsifying the data by keeping the peaks of the curves. For the shear relaxation tests, it was necessary to set the offset of the shear stresses at the beginning of the experiment to zero, as otherwise this would eventually lead to false assumptions, as the height of the initial peak would be altered. Without this correction one could for example draw the conclusion that the corpus callosum is the stiffest region, which is not the case according to literature. As a result of this the comparison between each graph was possible.

## 2.6 Oedometer Test

Due to the fact that the brain not only consists of brain tissue and blood vessels, but also fluid such as the cerebrospinal fluid, it is insufficient to try to characterize the mechanical behavior of the brain solely based on viscoelastic tests, because such experiments do not include the flow of fluids through the porous medium [Tada et al., 1994]. Hence, it is necessary to consider the brain parenchyma as a fluid saturated porous material, as otherwise a correct description of several diseases such as brain edema or hydrocephalus were impossible [Sivaloganathan et al., 2005] [Franceschini et al., 2006].

Therefore, additionally to the experiments, a literature research was conducted on how the poroelastic behavior of the brain tissue could be determined. It is based on the theory of consolidation, which was initially developed in soils mechanics, as described in Biot [1941].
But what does the word consolidation mean?
According to literature consolidation is defined as the procedure, whereby the pore volume decreases, due to the outflow of the fluid, as the tested tissue relaxes under a specific load [MacMinn et al., 2016]. Even though the theory has found significant applications in the field of biomechanics for example in the flow through cartilage or intervertebral disc as described in Oloyede and Broom [1991] and Martinez et al. [1997], only few studies were applied for brain tissue or other soft biological tissue [Franceschini et al., 2006].

Due to the fact that some studies described the brain parenchyma as a fluid saturated porous material, the consolidation theory has also been applied to brain biomechanics [Franceschini et al., 2006]. Their main objective was to describe and understand the fundamental mechanical behavior of the onset of diseases such as brain edema and hydrocephalus [Tada et al., 1994] [Kaczmarek et al., 1997]. However to be able to examine the poroelastic properties of brain parenchyma, it is necessary to use a uniaxial strain apparatus with free drainage that enables the execution of the oedometer test as described in Franceschini et al. [2006]. With the aid of this test it was possible to measure the consolidation properties of a soil, which was originally used in geotechnical engineering.

A testing device that is capable to perform these tests can be seen in Franceschini et al. [2006]. For this apparatus it is important that the device is composed of metallic constituents. Before the experiments start one has to mount the specimen in the testing device and subsequently load it with for example a cylindrical piston [Franceschini et al., 2006]. To be able to permit free drainage of the interstitial fluid it is necessary that the lower and upper part of the specimen is covered with filter paper, which have to be fixed on porous metal [Franceschini et al., 2006].

Due to the applied load, which results in a deformation of the solid matrix of the specimen, cerebrospinal fluid was squeezed out of the brain parenchyma, similar to a sponge saturated with water. This deformation which is typical for porous material, is called a process of consolidation [Terzaghi, 1943] [Stastna et al., 1999]. This led to a vertical deformation that needs to be recorded. It will be used to calculate for example the average consolidation ratio but also other important parameters, which are used to describe the poroelastic properties of the brain tissue. If the specimen was in a container filled with PBS, as it was the case for the oedometer test, and load is subsequently removed, the specimen will again absorb the fluid and expand, which would be the case for poroelastic materials [Terzaghi, 1943].

As described in Terzaghi [1943] the theory of consolidation consists of the following five assumption:

1. the soil is completely filled with fluid
2. solid constituents as well as the fluid are incompressible
3. equation of Darcy's law is valid
4. coefficient of permeability is constant
5. the delay of consolidation is based on the low permeability of the soil

With the help of the oedometric test the average consolidation ratio $U$ can be calculated. It is defined by the ratio between the instantaneous shortening of the sample and the final reduction of the specimen at the end of consolidation. Therefore the average consolidation

ratio ranges between 0 and 1 [Franceschini et al., 2006]. It can be calculated with the following equation:

$$U_z = 1 - \frac{p_w}{p_{w0}}. \tag{2.1}$$

With $p_w$ representing the pore volume and $p_{w0}$ the value of the pressure at the beginning of the experiment [Franceschini et al., 2006]. The results of the oedometric test could be compared to the prediction of the theory of Terzaghi. The main equation for the oedometric test is given by:

$$c_v \frac{\partial^2 p_w}{\partial z^2} = \frac{\partial p_w}{\partial t}, \tag{2.2}$$

with $z$ representing a space variable, $t$ a time variable and $c_v$ the coefficient of consolidation. It is defined by the rate where the consolidation process resumed and it was given by the following equation:

$$c_v = \frac{kM}{\gamma_w}. \tag{2.3}$$

Equation 2.3 consists of the parameters $k$, $M$ and $\gamma_w$, which describe the permeability $k$, elastic oedometric coefficient $M$ and the specific weight of the saturating fluid $\gamma_w$.
Due to the fact that such a testing device was not available during the performance of this thesis, this literature review was conducted to describe a testing device capable to determine the poroelastic properties of brain tissue.

# 3 Results

## 3.1 Simple Shear Test

For the results presented in this chapter, a total of one human and five porcine brains were used. The first graphs depict the results of the cyclic simple shear tests. This experiment was used to analyze the viscoelastic and nonlinear behavior of the brain tissue. Figure 3.1 depicts the simple shear test of one porcine brain sample. As described in Budday et al. [2017a], the tissue revealed an obvious hysteresis and a nonlinear behavior. The hysteresis, which is one of the main characteristics of viscoelastic materials, can clearly be seen in Fig. 3.1.

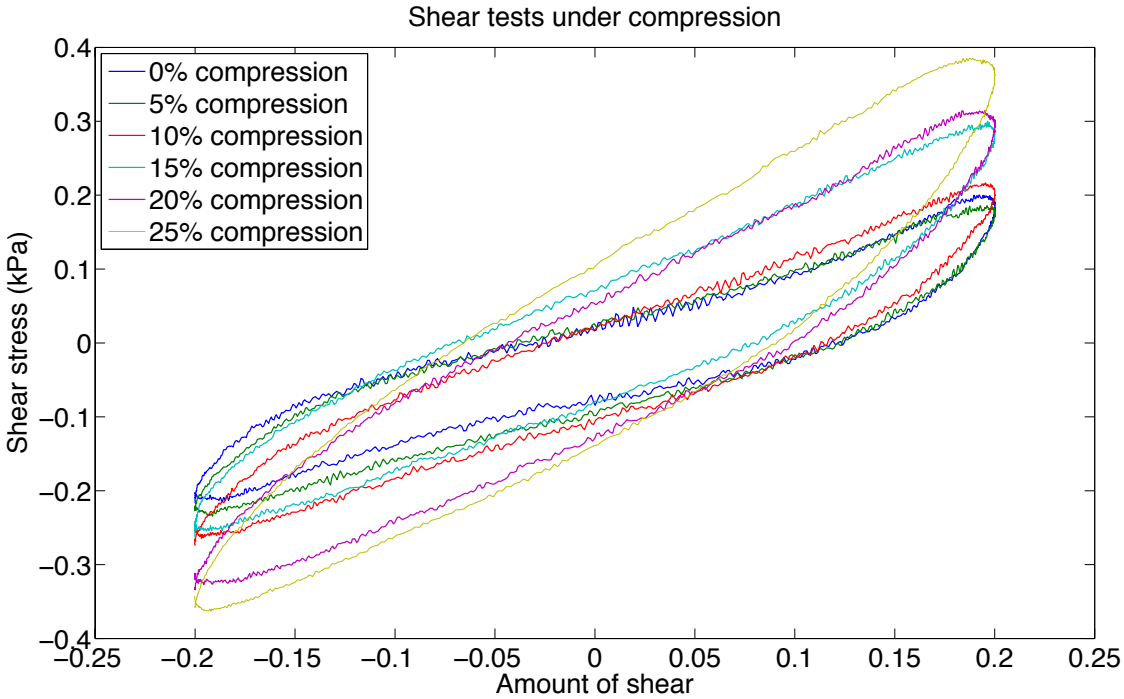


Figure 3.1: Shear stress vs. amount of shear behavior of a porcine brain sample of the white matter. This graph depicts the results of the simple shear test under different compression strains starting from 0% to a max. of 25% compression. This plot also depicts the viscoelastic behavior, which can for example be seen in the big hysteresis formed during cyclic shearing.

Compared to the typical shape of a hysteresis, it can be seen that the results of the simple shear experiments in Fig. 3.1 did not exhibit sharp edges at the end of each shearing process, but smooth ones. The reason for that was, that due to the sinusoidal movement the strain rate decreased at the end of each shearing process, which led to smooth edges. This figure also indicates that the shear stresses increased with increasing compression strain, as described in Pogoda et al. [2014] and Budday et al. [2017a]. The reason for that was that due to the compression force, the compactness of the solid constituents increased, which led to an increase in friction between these constituents which finally resulted in an augmentation of the shear stress.

Figure 3.2 depicts further results of the simple shear tests under tension. In this graph it can be seen that the shear stresses under tension were lower compared to the results from Fig. 3.1. Since the shear stress increased with increasing compression strain, it would be obvious to assume that the opposite behavior occurs under tension, because under tension the compactness of the solid constituents decreased, which resulted in less friction and a decrease of the shear stress.

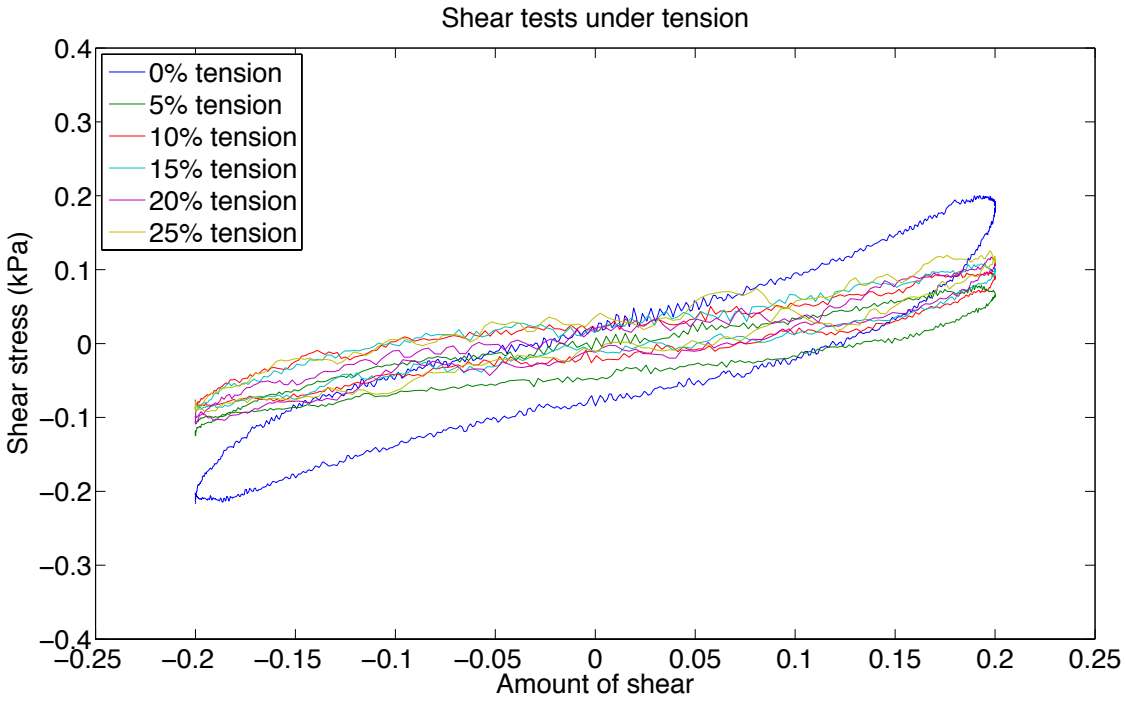


Figure 3.2: Shear stress vs. amount of shear behavior of a porcine brain sample of the white matter. This graph depicts the results of the simple shear test under tension starting from 0% to a max. of 25% tension strain. It can also be seen that the maximum shear stresses under tension stayed more or less the same.

But as can be seen in Fig. 3.2 the shear stress stayed more or less the same independent of the tension rate, which has already been established in literature by Budday et al. [2017a]. One possible explanation for this could be that the shear stresses were close to the resolution of the load cell and therefore no obvious alterations could be seen.

Figures 3.3 and 3.4 depict the simple shear tests for one human brain sample of the corona radiata, which was obtained from the Medical University Graz. The corona radiata consists of white matter with less aligned nerve fibers. As mentioned before the main characteristic of viscoealstic materials, is the hysteresis, which can be seen in the Figs. 3.3 and 3.4.

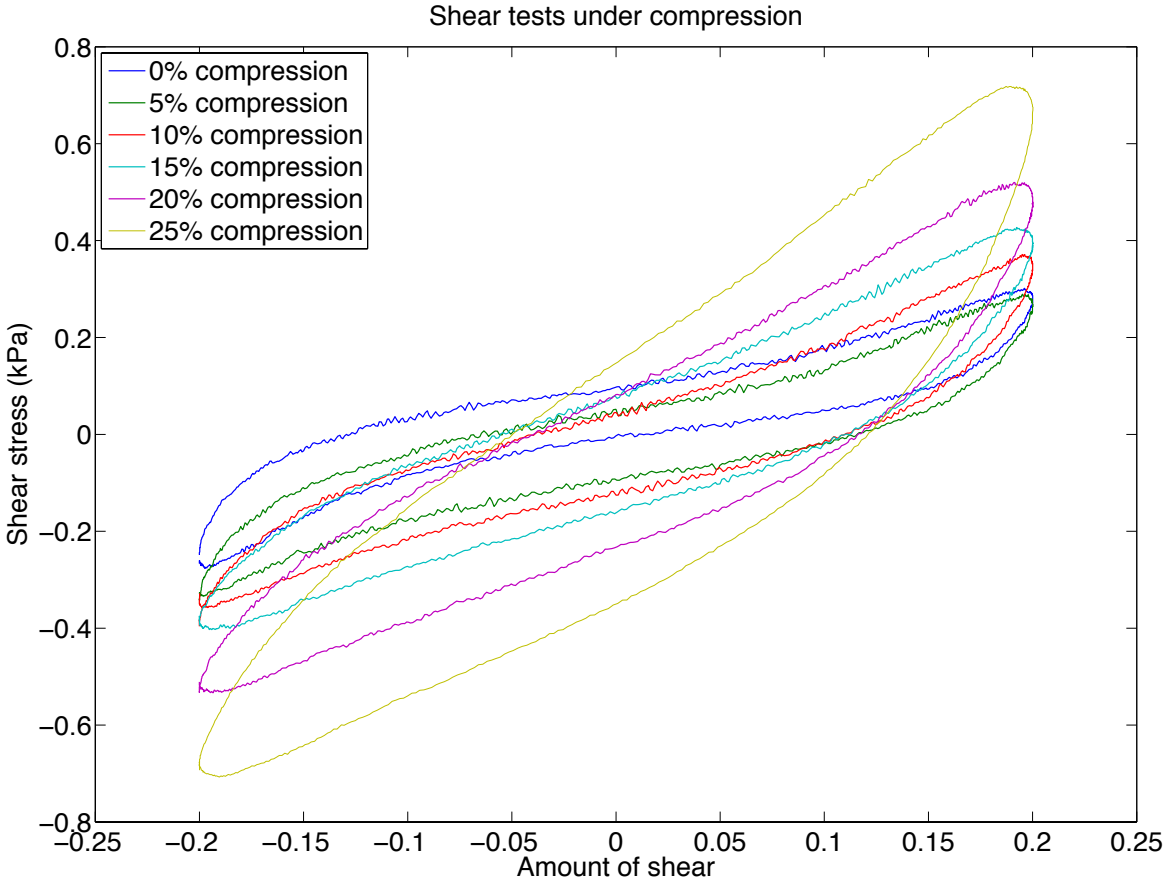


Figure 3.3: Shear stress vs. amount of shear behavior of human brain sample of the corona radiata. In this figure it can be seen that the shear stresses increased with increasing compression strain.

The results of the experiments represented in these figures show that the shear stresses increased with increasing compression strain and stayed more or less the same under tension, which coincides with the theory of Budday et al. [2017a] and Pogoda et al. [2014].

Figure 3.4 depicts the results of the simple shear experiments under tension. Compared to Fig. 3.3, it can be seen that the shear stresses under tension were smaller than the one under compression, which also coincides with the theory. The consistent shear stresses, which can be observed in Fig. 3.4, could result due to the fact that the stresses were close to the resolution of the load cell and therefore no obvious alteration could be seen. Another possible explanation could be that the specimen was saturated with PBS, as it was covered in it during the whole experiment, to prevent dehydration.

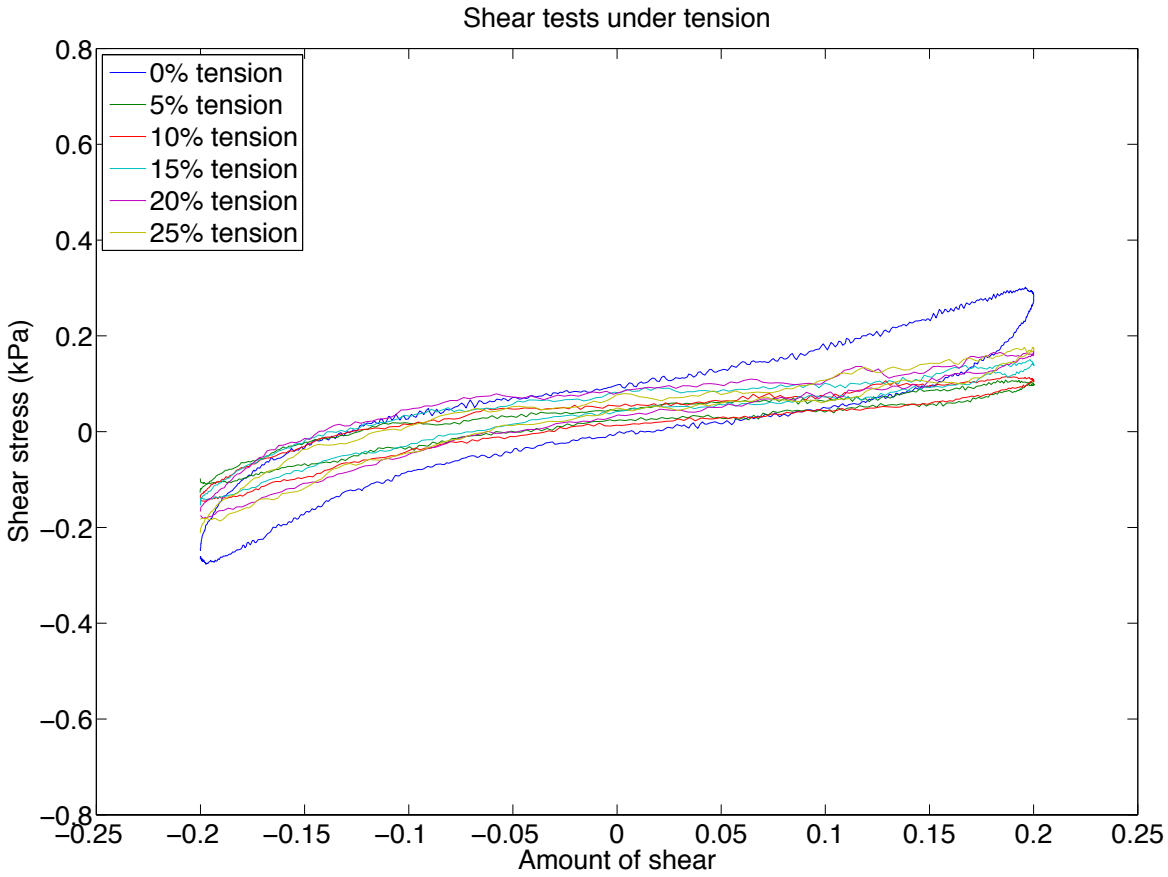


Figure 3.4: Shear stress vs. amount of shear behavior of human brain sample of the corona radiata. In this figure it can be seen that the shear stresses did not exhibit a decrease.

In comparison to the results of the trials from porcine samples, it can be seen that both porcine and human brain tissues behave very similar regarding the simple shear tests. One obvious distinction was the resulting shear stress, which was higher for human brain samples than for porcine samples.

This study was also used to analyze the regional dependency of the mechanical properties of the human brain tissue. Therefore these tests were conducted on the following regions: corpus callosum, basal ganglia, corona radiata and the cortex. Figures 3.5 and 3.6

depict the results of the cyclic simple shear tests of the corpus callosum, which also consists of white matter. Figure 3.5 shows that the obtained maximum shear stresses from the corpus callosum were smaller than the corresponding stresses from the corona radiata, which has already been described in Budday et al. [2017a]. It can also be seen that the curves in this graph perfectly represent the viscoelastic and nonlinear behavior, as shown by the big hysteresis area.

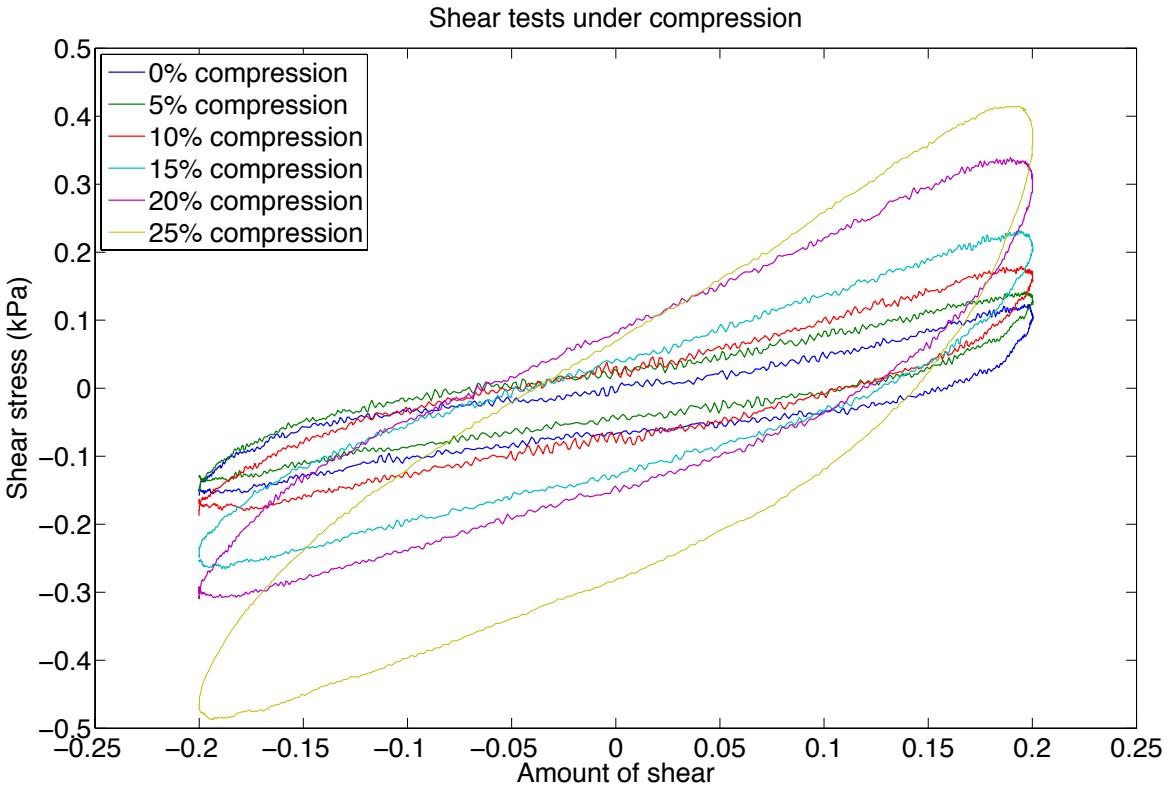


Figure 3.5: Shear stress vs. amount of shear behavior of human brain sample of the corpus callosum. The increase of the shear stresses is evident in this graph. It also depicts the nonlinear and viscoelastic time response, which is represented by the big hysteresis area.

Compared to the results of Fig. 3.6, it can be seen that the shear stresses under compression are higher than under tension, which coincides with the theory. Figure 3.6 also depicts that the shear stresses under tension did not increase. Even though the shear stresses from Fig. 3.4 of the corona radiata are higher than the one from the corpus callosum, it can be seen that under tension they closely resemble each other. Again, the reason for that could be the limited resolution of the load cell or that the specimen was saturated with PBS.

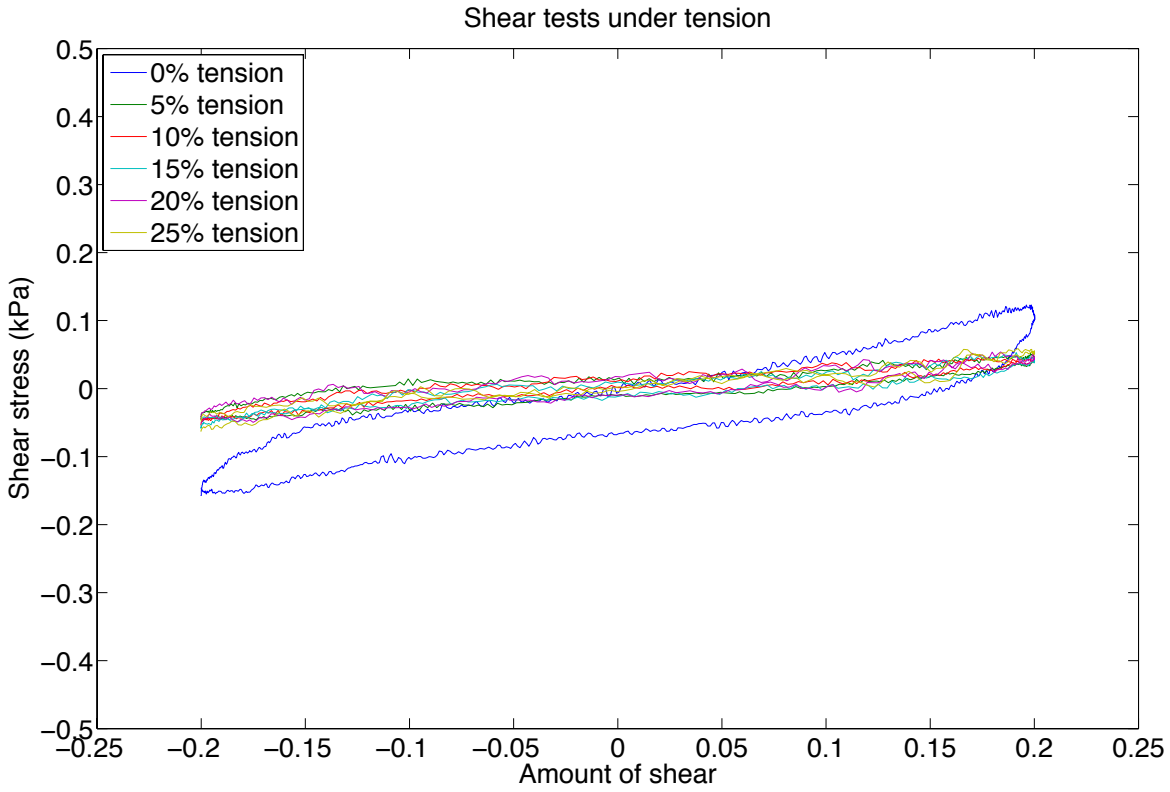


Figure 3.6: Shear stress vs. amount of shear behavior of human brain sample of the corpus callosum. It depicts the slightly nonlinear and viscoelastic behavior of the tissue, represented by the formation of a hysteresis area. This figure exhibits that the shear stress did not increase with increasing tension.

Figures 3.7a and 3.7b represent the results of the simple shear experiments from the basal ganglia. The basal ganglia consists of the inner gray matter. Compared to the results of the previous regions, it can be seen that the basal ganglia are stiffer than the corpus callosum. Under closer examination it can be seen that the maximum shear stresses under 25% compression were higher for the corona radiata than the basal ganglia, but the shear stresses at lower compression rates tend to be higher for the basal ganglia. This leads to the assumption that the basal ganglia are stiffer than the corona radiata under low strain rates, as it is the case for the simple shear experiments. Figure 3.7b depicts the results of the trials under tension. In this graph it can also be seen that the shear stresses under tension are slightly higher than the one from the corpus callosum. Furthermore it depicts that the shear stresses, starting from 5% tension, did not exhibit obvious alterations with increasing tension strain.

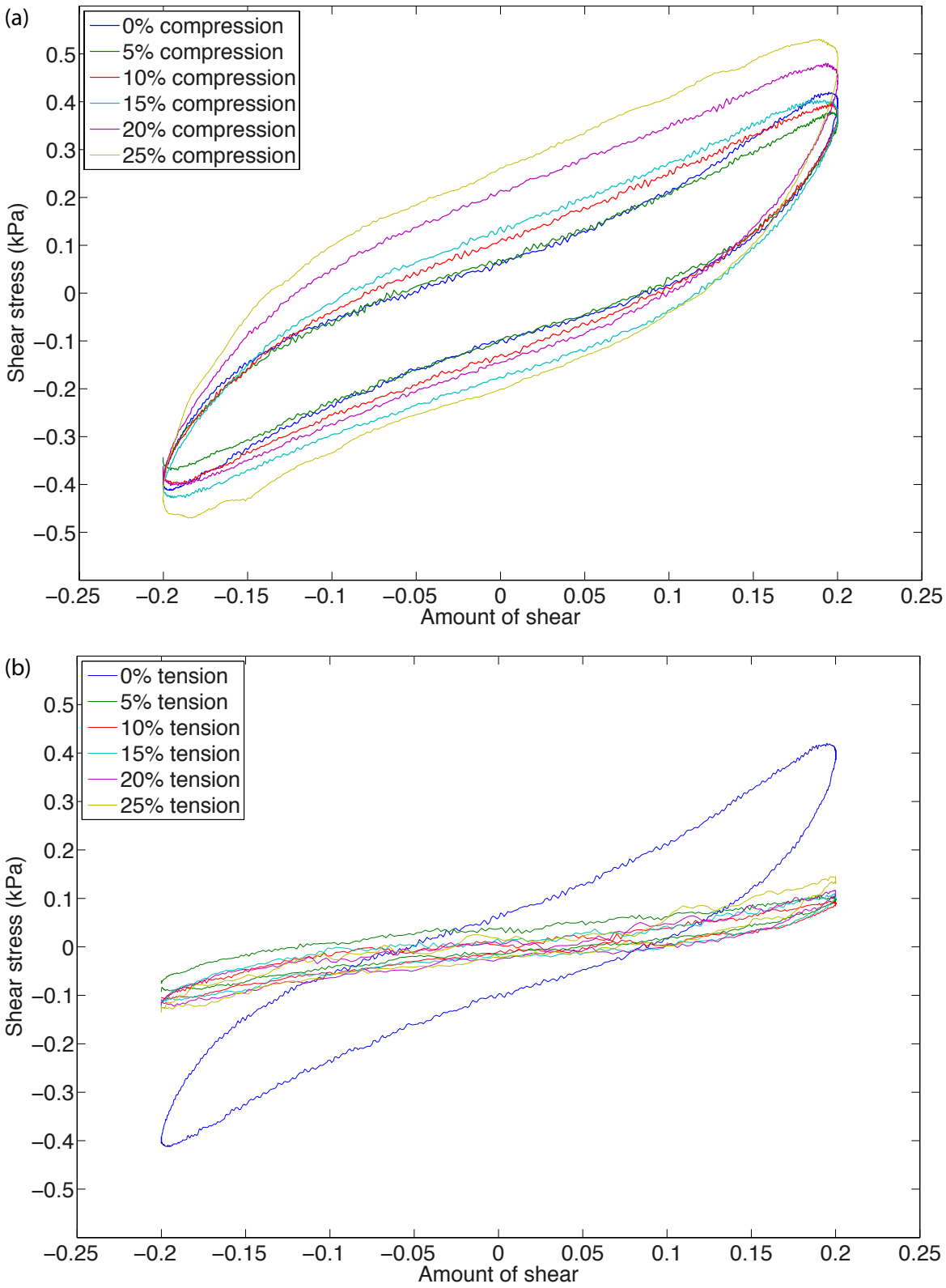


Figure 3.7: Shear stress vs. amount of shear behavior of human brain sample of the basal ganglia under compression (a) and tension (b). It depicts the nonlinear and viscoelastic behavior of the tissue, represented by the formation of a hysteresis area.

Figures 3.8 and 3.9 depict the results of the simple shear experiments from the cortex. The cortex is the second region that consists of gray matter. It also exhibit nonlinear and viscoelastic behavior. Compared to the results of the basal ganglia, it can be seen that the cortex is slightly stiffer. Even though the maximum shear stresses at 25% compression from the corona radiata were marginally higher than the one from the cortex, it can be seen that the cortex is slightely stiffer compared to the other regions, as described in Budday et al. [2017a] and Budday et al. [2017b]. On closer inspection, it can also be observed that the specimens from the corpus callosum were the softest, which coincides with literature [Budday et al., 2017a] [Budday et al., 2017b].

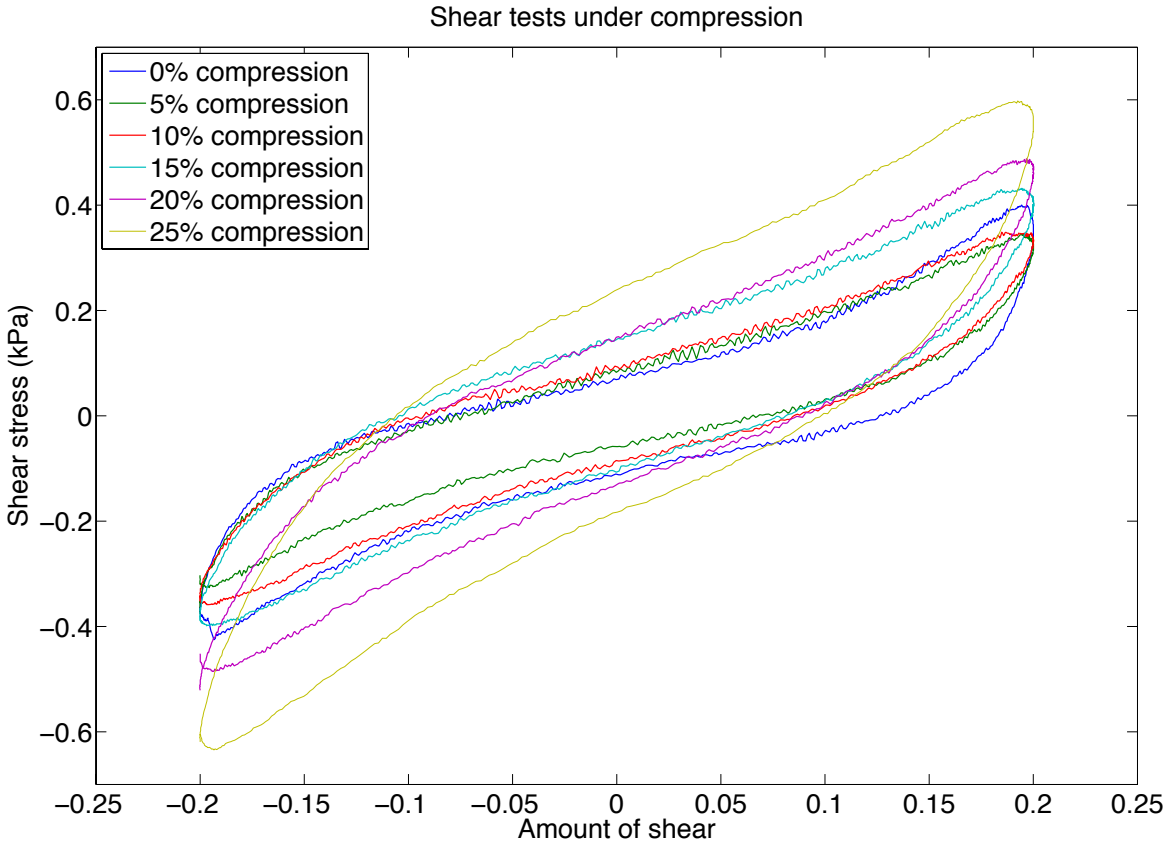


Figure 3.8: Shear stress vs. amount of shear behavior of human brain sample of the cortex. Compared to the results of the other regions it can be seen that the cortex is the stiffest one.

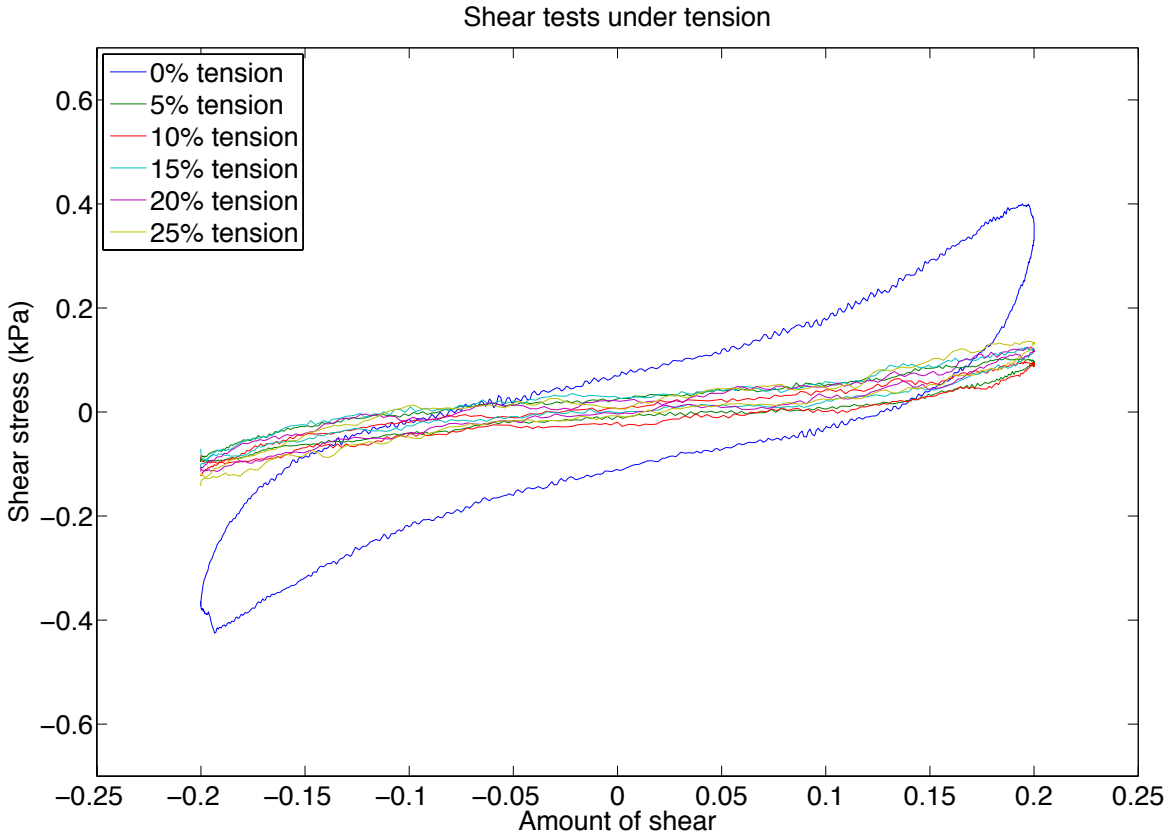


Figure 3.9: Shear stress vs. amount of shear behavior of human brain sample of the cortex. It can also be seen that there are no obvious alterations of the shear stresses starting from 5% tension.

To simplify the comparison between each region and to achieve a better insight in the regional dependency of the human brain tissue, all four brain regions were plotted in one graph for each loading rate. Figure 3.10 depicts the results of the simple shear experiments under compression. According to literature gray matter tissue was found to be stiffer than white matter, which can also be seen in Figs. 3.10 to 3.12 [Budday et al., 2017b]. Comparing both white matter tissues, the corpus callosum and the corona radiata, it can be seen that the latter one tends to be stiffer in shear. Under close examination, it can be seen that the cortex is the stiffest and that the corpus callosum is the softest region under low strain rates, which is demonstrated in Figs. 3.10 to 3.12.

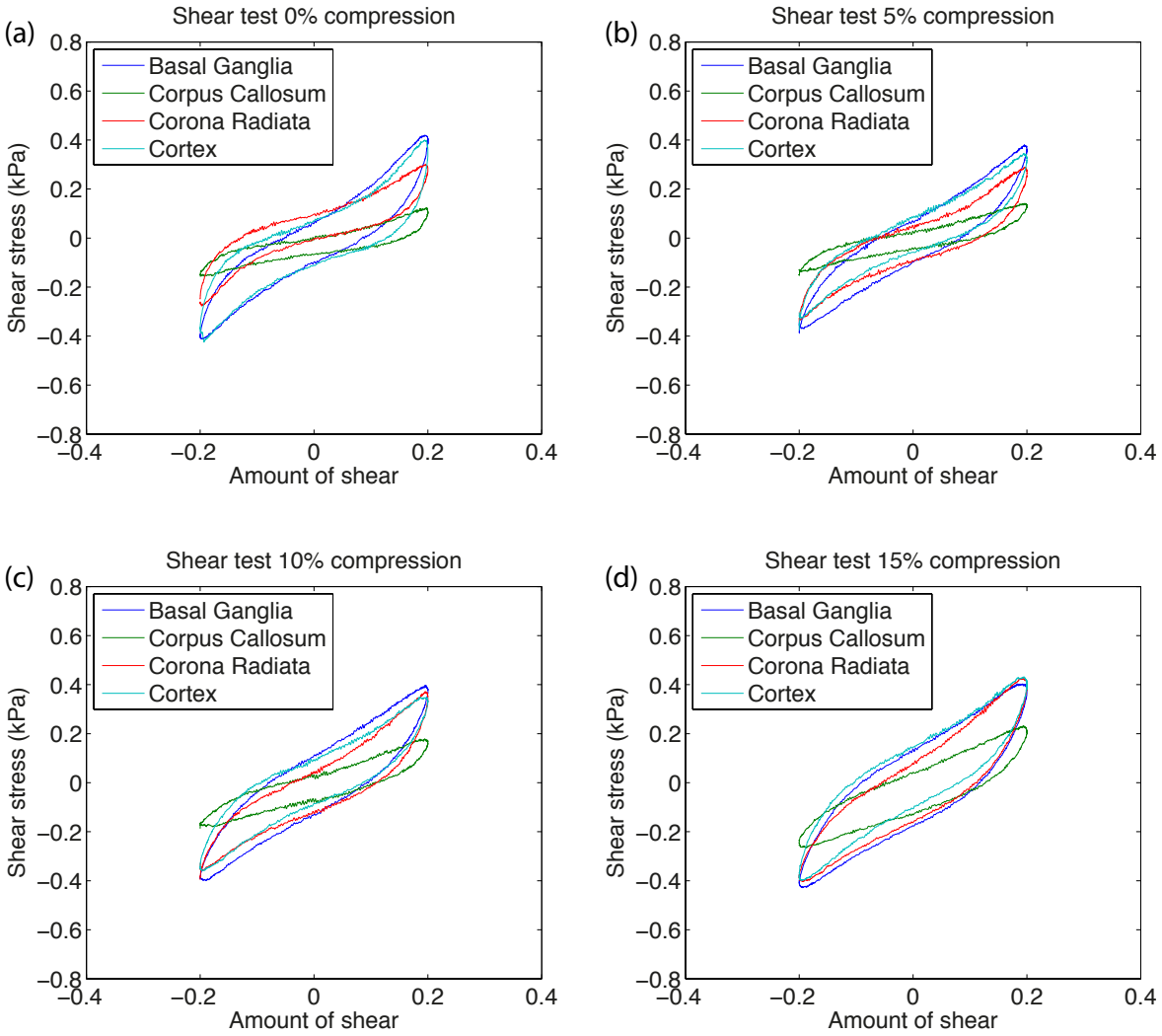


Figure 3.10: Shear stress vs. amount of shear behavior of human brain tissues from different regions, the basal ganglia, the corpus callosum, the corona radiata and the cortex at different compression strains (a)-(d). According to the figure it can be seen that the gray matter tissue (basal ganglia, cortex) seems to be stiffer than the white matter (corona radiata, corpus callosum) under slow strain rates. It also depicts that the corpus callosum is the softest region and that the cortex seems to be slightly stiffer than the basal ganglia.

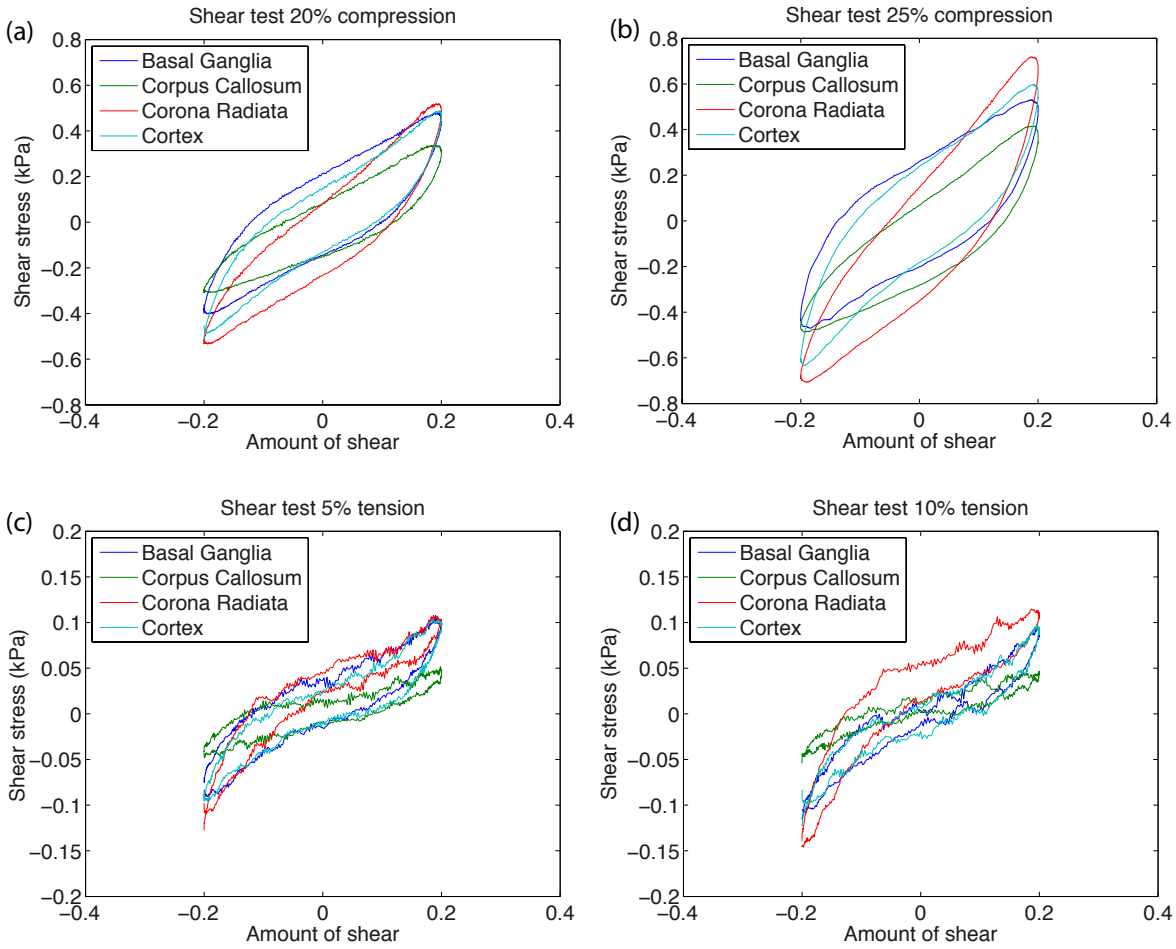


Figure 3.11: Shear stress vs. amount of shear behavior of human brain tissues from different regions, the basal ganglia, the corpus callosum, the corona radiata and the cortex at different compression (a)-(b) and tension strains (c)-(d). According to the figure it can be seen that the gray matter seems to be stiffer than the white matter under slow strain rates.

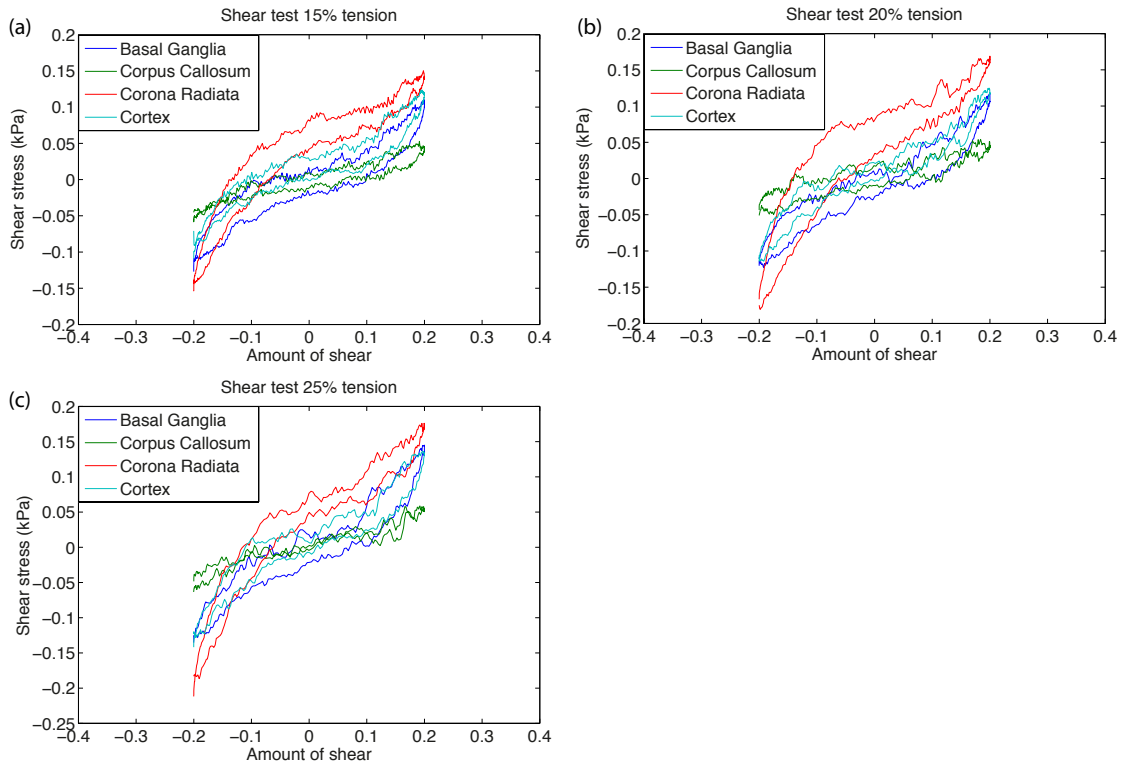


Figure 3.12: Shear stress vs. amount of shear behavior of all four tested regions from the human brain at different tension strains (a)-(c). It enables the comparison of the different brain regions. According to the figure it can be seen that the gray matter seems to be stiffer than the white matter.

## 3.2 Shear Relaxation Test

This chapter represents the results of the shear relaxation experiments. The idea was to achieve a better and more profound understanding of the viscoelastic behavior of the brain tissue. Therefore it was necessary to conduct shear relaxation tests at different compression and tension strains. In Fig. 3.13 the results of the shear relaxation tests of one porcine sample at different compression strains can be seen.
A good example of the stress relaxation behavior can be seen in the curves of Fig. 3.13.

It can also be seen that the shear stress increased with increasing compression rate. The reason for that was that due to the compression force, the compactness of the solid constituents increased, which led to an increase in friction between these constituents which finally resulted in an augmentation of the shear stress. This graph also depicts the viscoelastic behavior of the brain tissue, as the ratio between the maximum shear stress peak and the shear stress equilibrium was quite high.

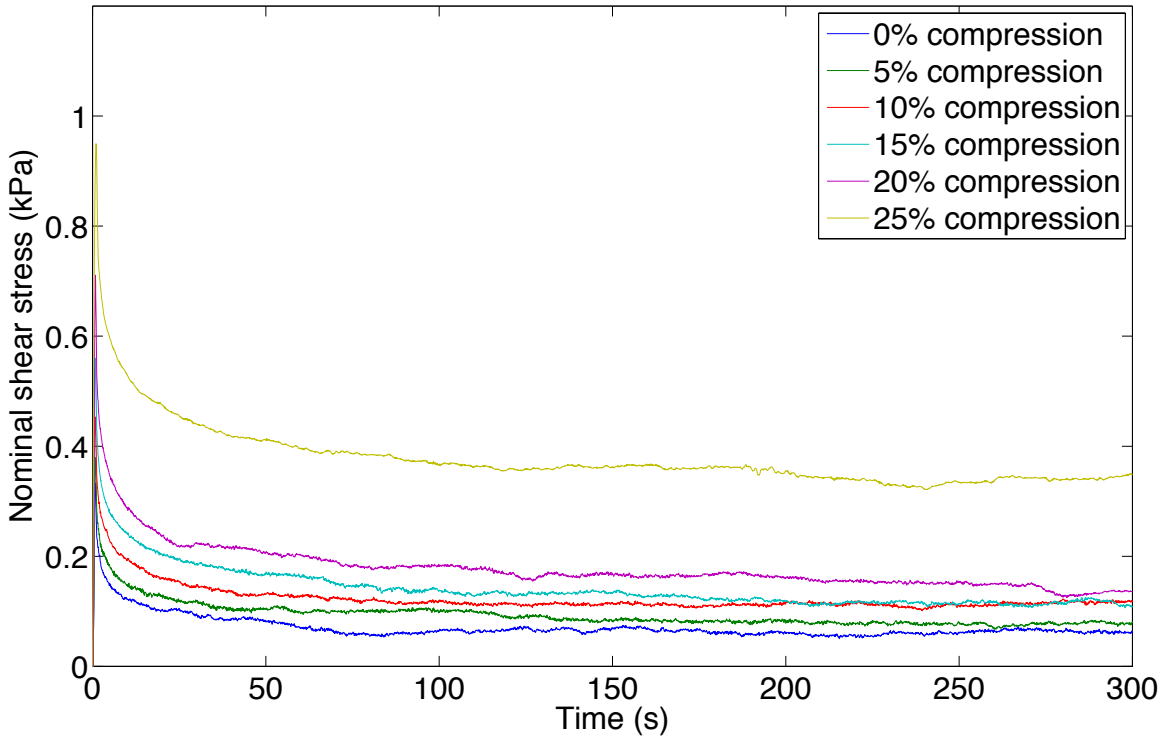


Figure 3.13: Nominal shear stress vs. time of a representative porcine brain specimen of the white matter. This graph depicts the results of the shear relaxation experiments under different compression strains starting from 0% to the max. of 25% compression. It also depicts the viscoelastic behavior, which can for example be seen in the yellow curve at 25% compression.

In Fig. 3.13 it can be seen that the initial stress values are higher compared to the results of Fig. 3.1. Directly after the initial peak of the shear stress a rapid relaxation process took place, which can for example be seen in the magenta curve of Fig. 3.14 and in the yellow curve of Fig. 3.13. This relaxation process slowly decreases until a shear stress equilibrium was achieved, which can be seen in the curves of Fig. 3.13. Figure 3.14 depicts the results of the shear relaxation experiments under different tension rates. Compared to the results under compression it can be seen that the shear stresses under tension were much lower, because under tension the compactness of the solid constituents decreased, which resulted in less friction and a decrease of the shear stress.

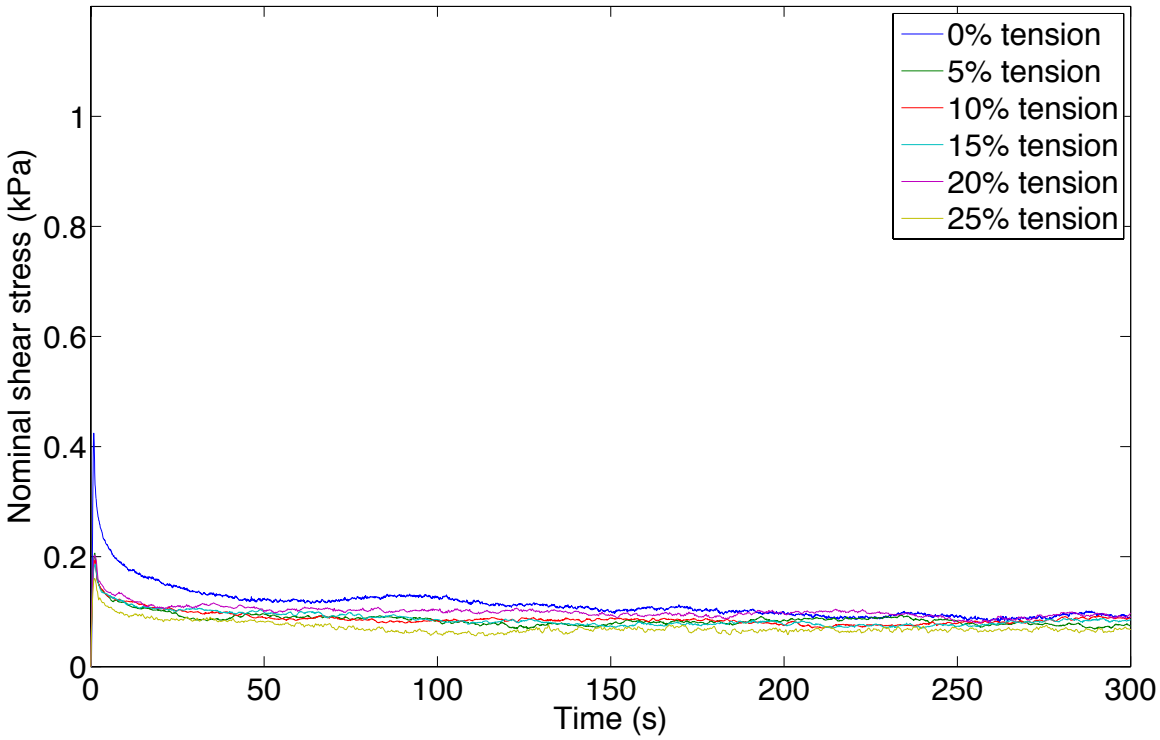


Figure 3.14: Nominal shear stress vs. time of porcine brain specimen of the white matter. This graph depicts the results of the shear relaxation experiments under different tension strains starting from 0% to the max. of 25% tension. It also depicts that the shear stresses are much smaller compared to the results under compression.

Close examinations of Fig. 3.14 reveal that the shear stress at 25% tension was the smallest. One possible explanatin for this could be that tension injuries of axons occur at 18% tension strain, as described in Bain and Meaney [2000]. This might lead to the assumption that the tissue got damaged during the experiments, which resulted in a decrease of the shear stress with increasing tension strain.

Figures 3.15 and 3.16 depict the results of the shear relaxation tests of the human corona

radiata under compression and tension, respectively. Figure 3.15 shows the viscoealstic behavior of the human brain tissue. It can also be seen that directly after the initial peak of the shear stress a rapid relaxation process takes place, as it was the case for the porcine specimens in Fig. 3.13. Compared to the results of Fig. 3.13, of the porcine sample, it can be seen that the shear stresses of the human sample from Fig. 3.15 were higher.

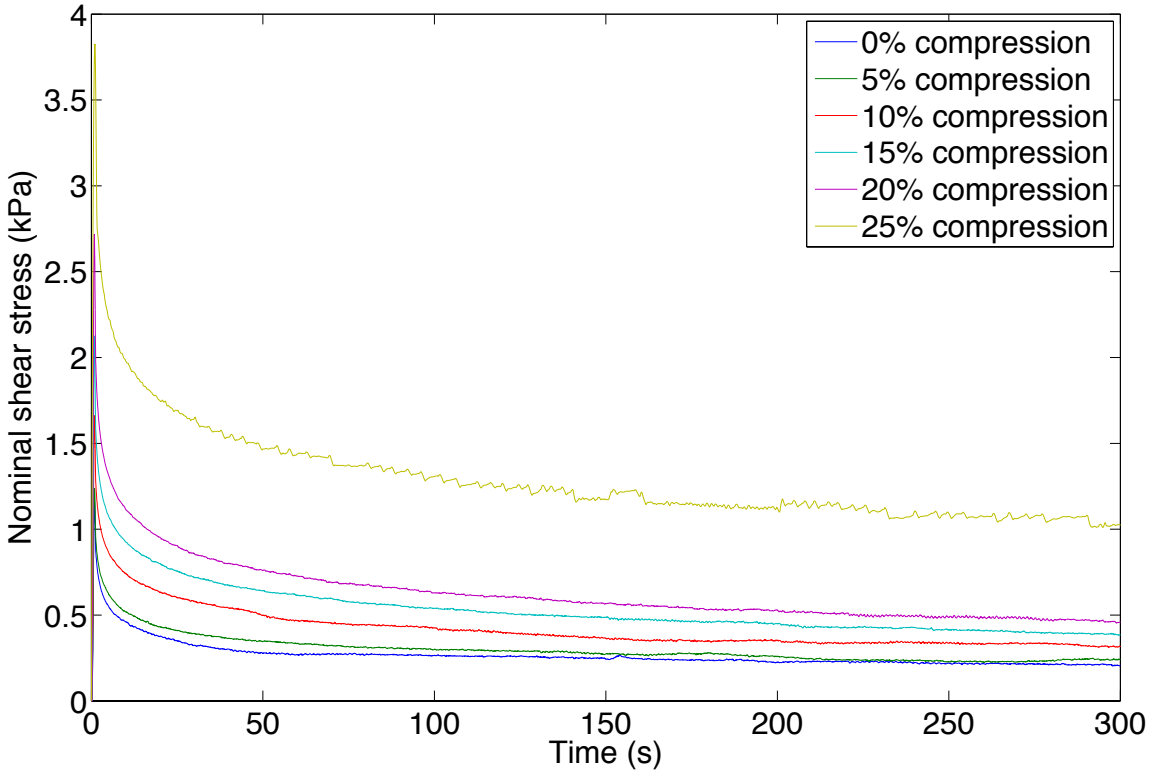


Figure 3.15: Nominal shear stress vs. time of the corona radiata from a human brain specimen. This graph depicts the results of the shear relaxation experiments under different compression strains starting from 0% to a maximum of 25% compression.

Figure 3.16 shows the results of the shear relaxation tests of the corona radiata under tension. It can be seen that the shear stresses under tension were much lower than under compression, as it was for the porcine samples. This plot also depicts very low shear stresses. The reason for that could be that the sample was drained in PBS due to the long duration of the experiments.

Figures 3.17a and 3.17b depict the results of the shear relaxation experiments of the corpus callosum. The ratio between the maximum shear stress and the shear stress at the equilibrium was used to describe the viscoelastic behavior of the tissue. In Fig. 3.17b it can be seen that the shear stresses under tension were low, similar to the corona radiata of Fig. 3.16. At closer examination, this graph depicts the lowest shear stresses at 25%

tension. The reason for that could be due to the tension injuries of the axons, which occur at 18% tension strain, as described in Bain and Meaney [2000].

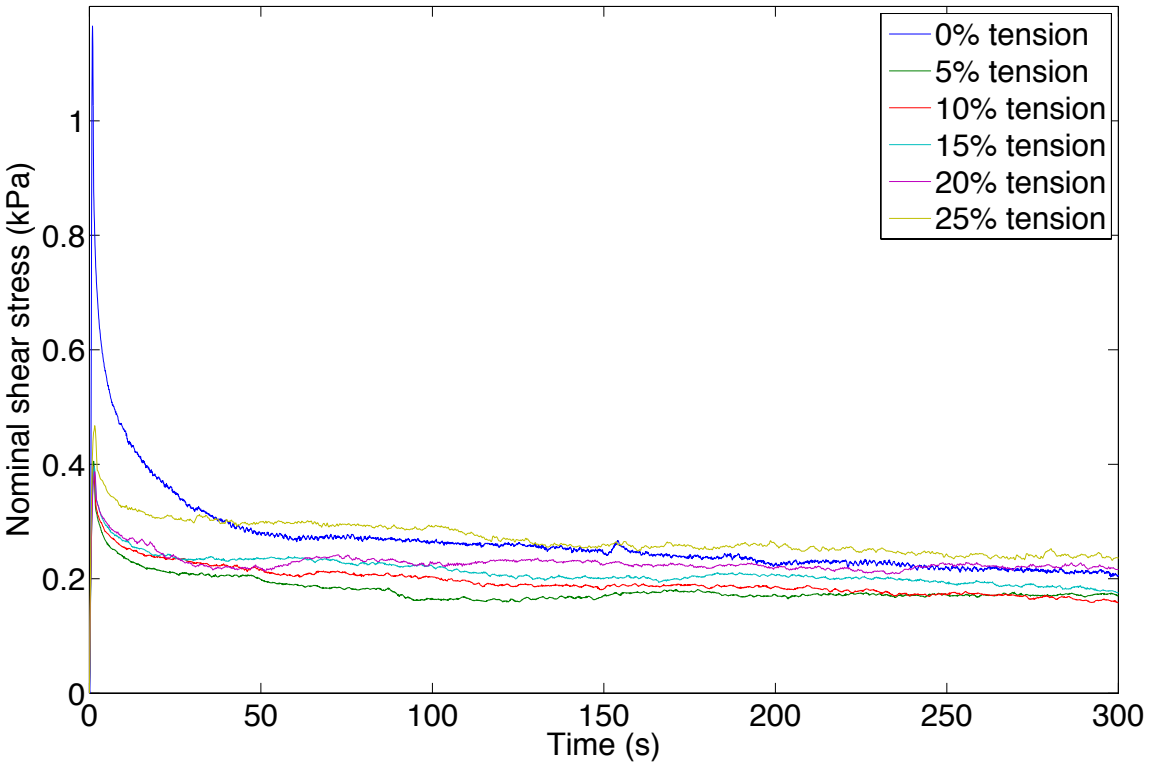


Figure 3.16: Nominal shear stress vs. time of the corona radiata from a human brain specimen. This graph depicts the results of the shear relaxation experiments under different tension strains starting from 0% to a maximum of 25% tension. It also depicts that the shear stress was much smaller compared to the results under compression.

The results of the relaxation experiments from the cortex can be seen in the Figs. 3.18a and 3.18b. Figure 3.18a represents the results under compression and 3.18b the one under tension. If compared to the results of the corona radiata it can be seen that the cortex exhibited lower shear stresses under compression.

Figures 3.19a and 3.19b depict the results of the relaxation experiments from the basal ganglia. In Fig. 3.19a it can be seen that the shear stresses did not exhibit a constant augmentation with increasing compression strain, which contradicts theory. One possible assumption could be that the nonlinear behavior of the brain tissue is more pronounced under compression than under tension.

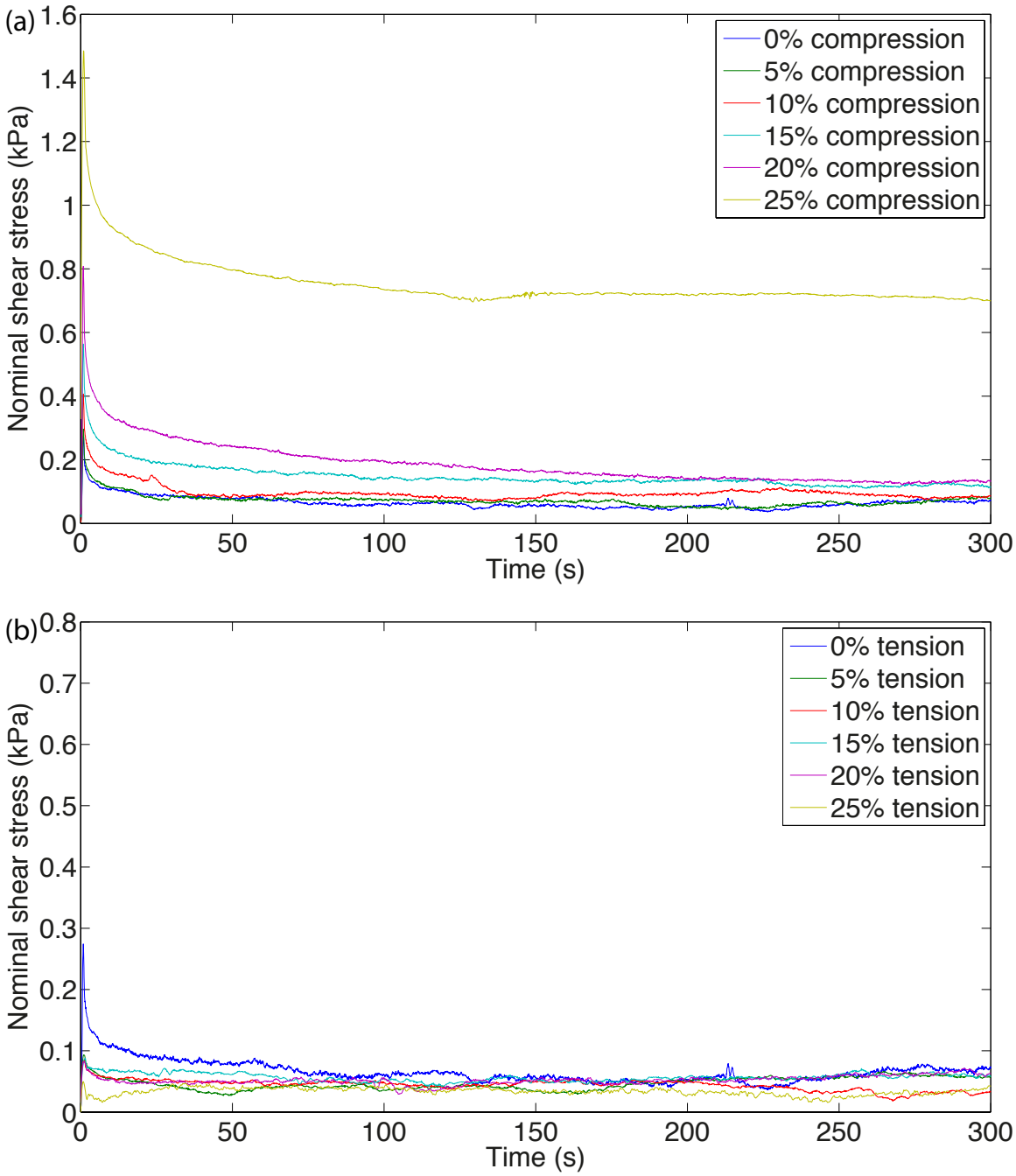


Figure 3.17: Nominal shear stress vs. time behavior of the corpus callosum from a human brain specimen. Graph in (a) depicts the results of the shear relaxation experiments under compression and graph in (b) the one from the same trials under tension.

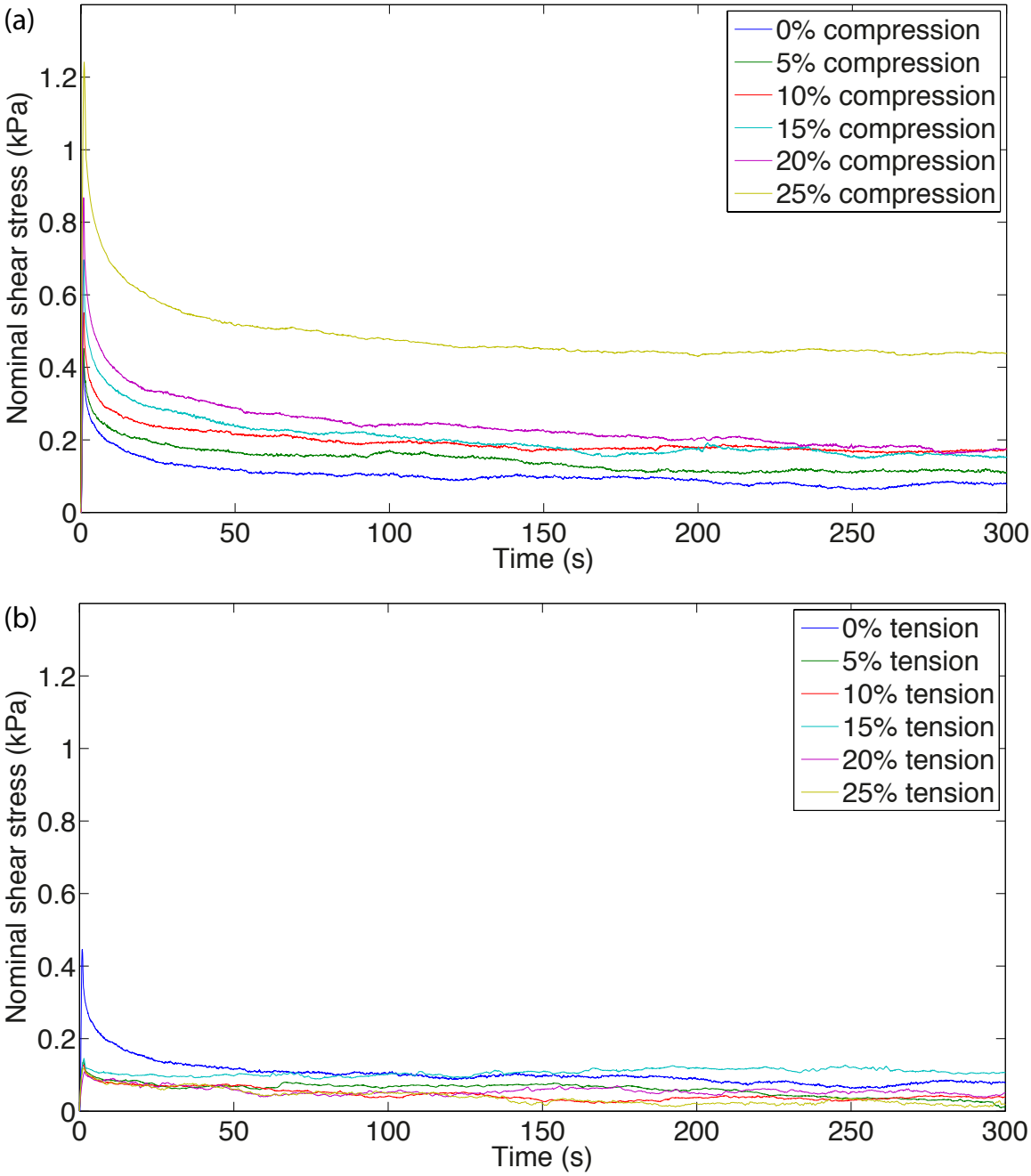


Figure 3.18: Nominal shear stress vs. time behavior of the cortex from a human brain specimen. Graph in (a) depicts the results of the shear relaxation experiments under compression and graph in (b) the one from the same trials under tension.

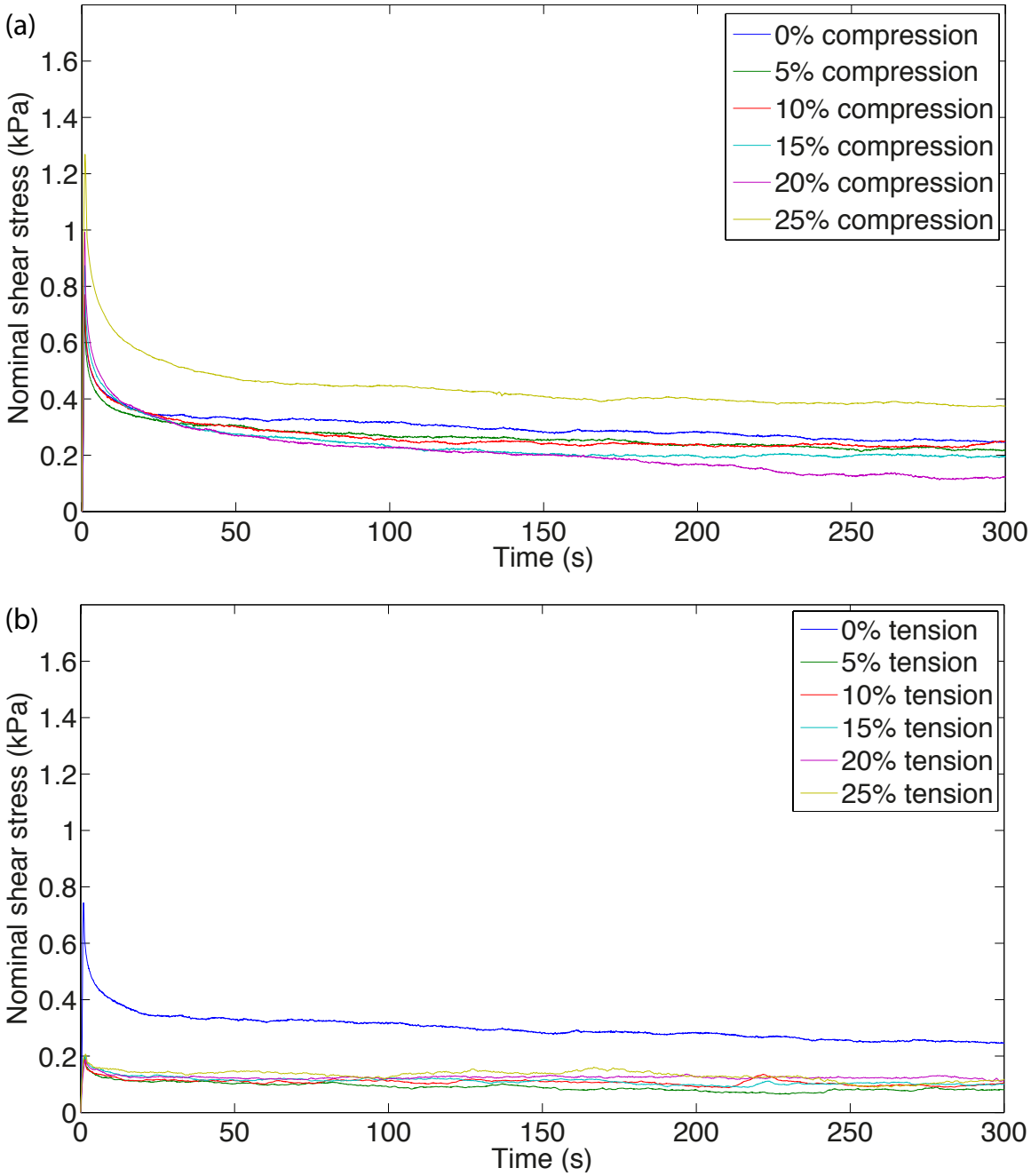


Figure 3.19: Nominal shear stress vs. time behavior of the basal ganglia from a human brain specimen. Graph in (a) depicts the results of the shear relaxation experiments under compression and graph in (b) exhibits the results from the same trials under tension.

Another possible explanation for this could be that the mechanical properties of the tissue started to degenerate with the increasing postmortem time due to for example autolytic

processes, completion of rigor mortis or osmotic swelling [Hrapko et al., 2008a], as this experiment was performed approximately four days after the autopsy.

For a better comparison between each brain region and to achieve a better insight in the regional dependency of the brain tissue, all regions were plotted together under each strain level. In Fig. 3.20 it can be seen that at low compression rates the corona radiata and the basal ganglia exhibit the same shear stresses, but with increasing loading rates the corona radiata seems to be stiffer. Therefore the assumption can be made that under fast loading conditions the corona radiata becomes the stiffest region, which agrees well with previous studies [Budday et al., 2017b] [Jin et al., 2013].

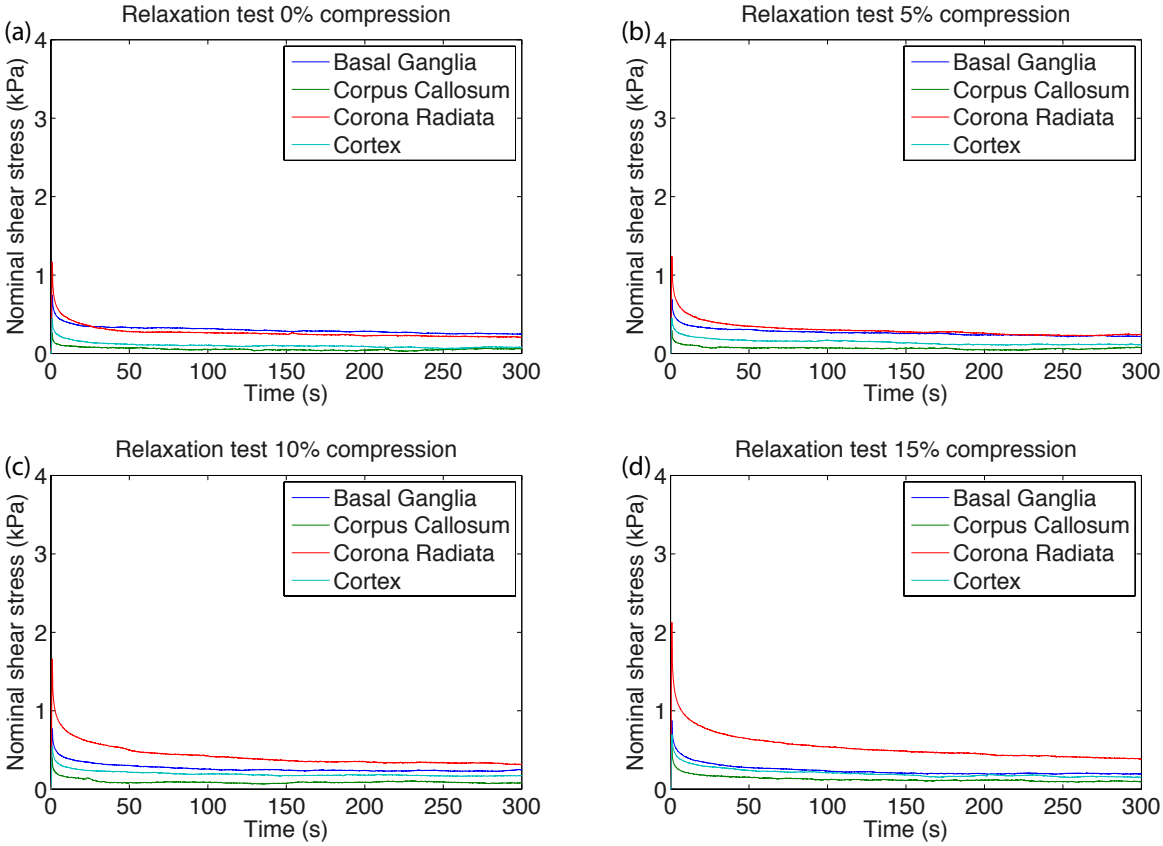


Figure 3.20: Nominal shear stress vs. time of all four tested regions from the human brain at different compression strains (a)-(d). This graph depicts the results of the shear relaxation experiments under different compression strains starting from 0% to 15% compression. It also depicts that the corona radiata becomes the stiffest region under fast loading rates.

Figure 3.21 also shows that the corona radiata is the stiffest region under fast loading rates. It additionally depicts the first two trials under 5% and 10% tension strain. Figure 3.22 represents the final results of the shear relaxations experiments under different tension strains. As shown in these Figures it can be observed that even under tension the corona radiata becomes the stiffest region and that the corpus callosum becomes the softest one for fast loading conditions [Jin et al., 2013] [Budday et al., 2017b].

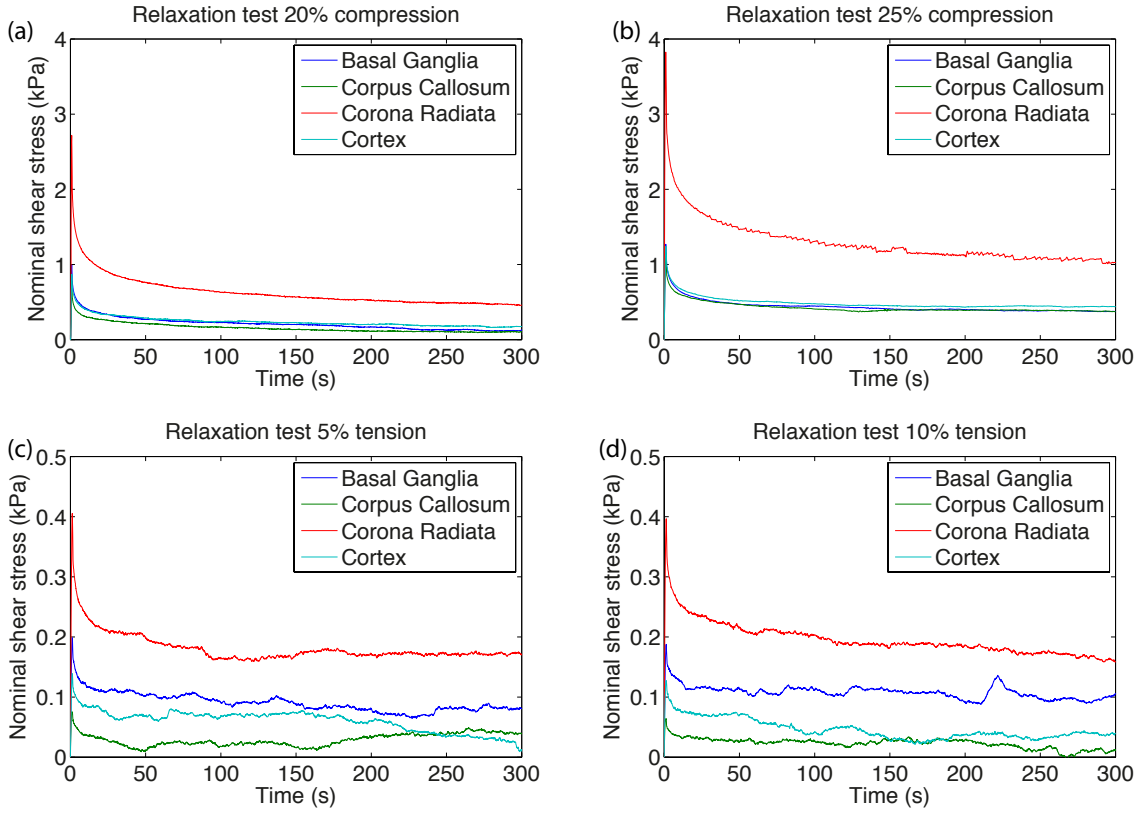


Figure 3.21: Nominal shear stress vs. time of all four tested regions from the human brain at different compression (a)-(b) and tension strains (c)-(d). This graph depicts the results of the shear relaxation experiments under different compression and tension strains. It also depicts that the corona radiata becomes the stiffest region under decreasing time scale.

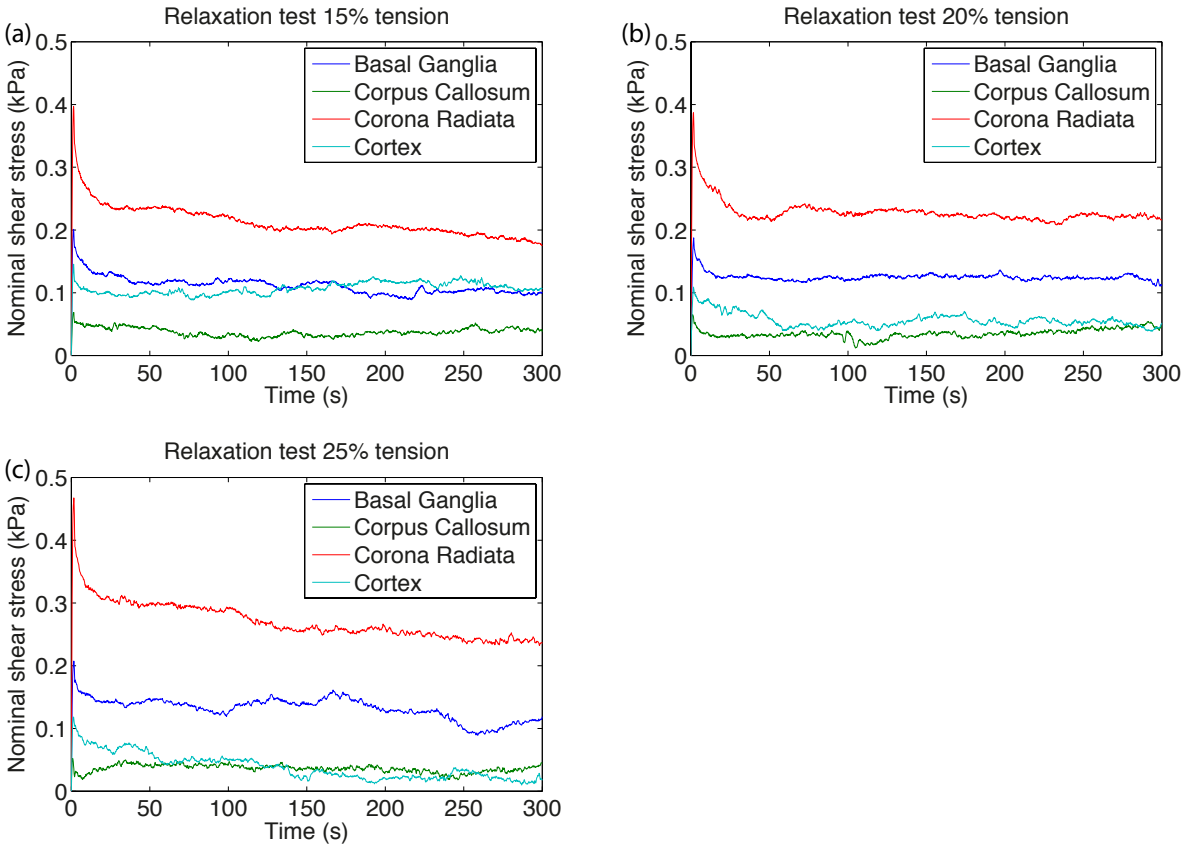


Figure 3.22: Nominal shear stress vs. time of all four tested regions from the human brain at different tension strains (a)-(c). This graph depicts the results of the shear relaxation experiments under different tension strains. It also depicts that the corona radiata becomes the stiffest region under fast loading rates.

### Different testing conditions

In addition to the shear relaxation experiments a few trials have been conducted under different testing conditions. Figures 3.23a and 3.23b represent the results of the experiments, where the specimen was only humidified with PBS. Here it can be seen that the augmentation of the shear stress starting from 10% compression strain is comparatively high, with respect to the lines of Fig. 3.13 where the specimen was covered in PBS. The reason for that was that due to the long duration of the experiment, the specimen started to dry out and the tissue became stiffer, which resulted in an increase of the shear stress. As shown in Fig. 3.23b, which represents the results of the same experiment under tension, the shear stress is much higher compared to the specimen that was covered in PBS of Fig. 3.14. The reason for that was that the specimen started to dehydrate due to the long duration of the experiment.

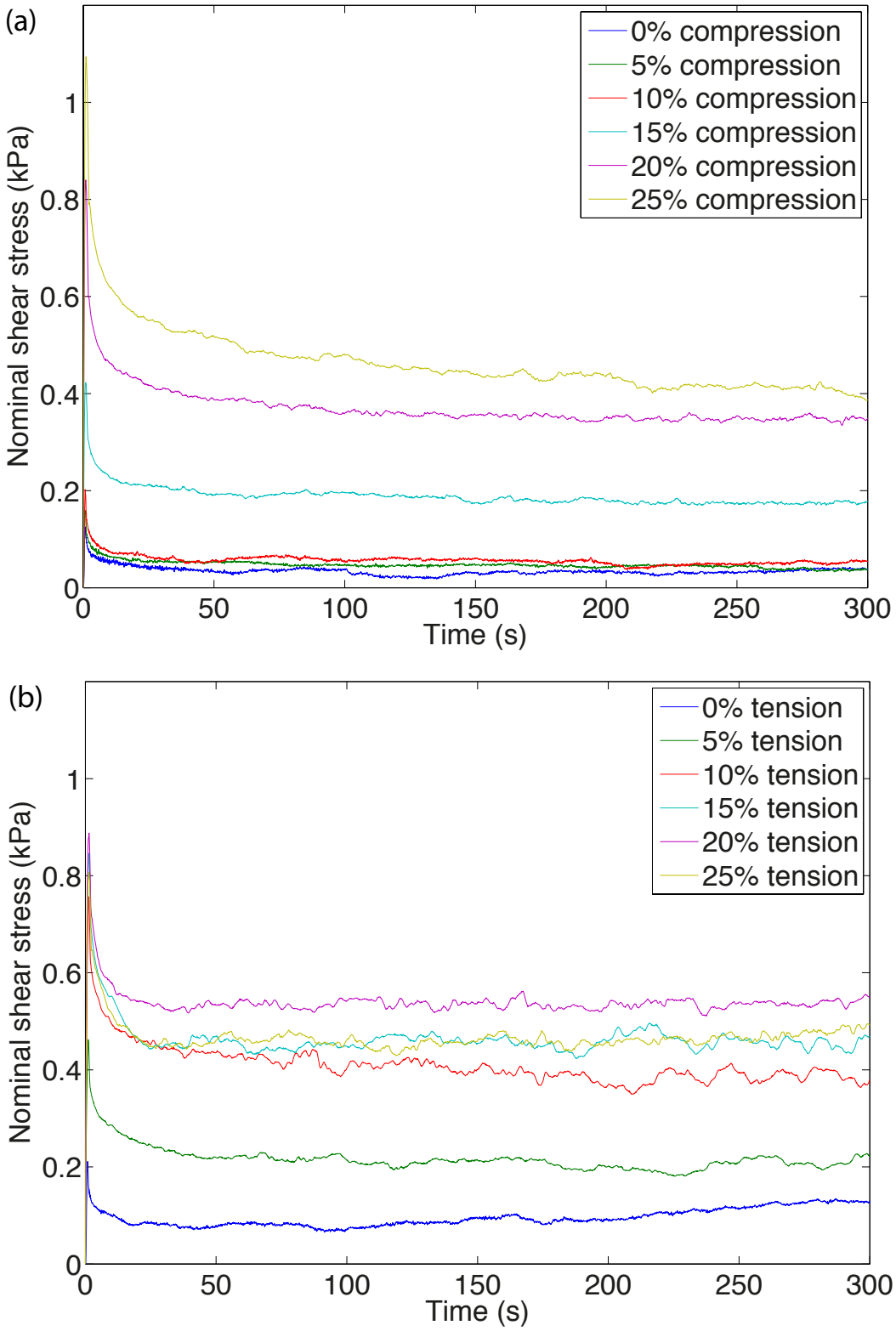


Figure 3.23: Shear relaxation experiments of one porcine brain sample, where the specimen was only humidified with PBS. Graph in (a) depicts the results of the shear relaxation experiments under compression and graph in (b) exhibits the results from the same trials under tension.

This graph also exhibits an increase in shear stress with increasing tension, which contradicts the theory, as the shear stresses should decrease with increasing tension strain, due to a decrease in the compactness of the solid constituent. Therefore it is necessary to fully cover the specimen with PBS, otherwise the mechanical properties would change with time, which would eventually lead to false assumptions. Consequently one could for example assume that the tissue is stiffer under tension than under compression. Under closer examination it can also be seen that the stress at 25% tension decreased compared to the one at 20% tension. The reason for that could be that tension injuries of the axons already occur at 18% tension, as described in Bain and Meaney [2000].

Figures 3.24 and 3.25 depict the results of the shear relaxation test in PBS and CSF. The idea was to investigate if the results in PBS differ from the one in CSF. The artificial cerebrospinal fluid was mixed according to the paper of Zhan and Nadler [2009]. Comparing these to graphs with each other, it can be seen that there are slightly differences between PBS and CSF, therefor it is not necessary to use CSF instead of PBS.

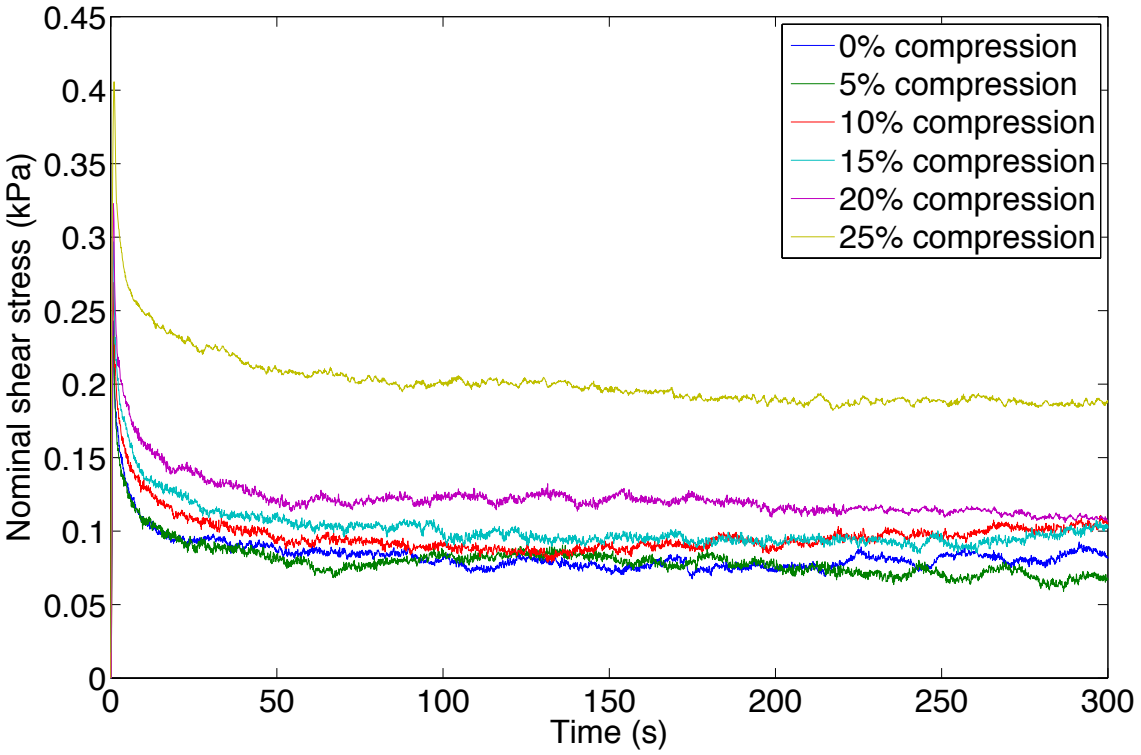


Figure 3.24: Nominal shear stress vs. time of one porcine brain sample tested in PBS. This graph depicts the results of the shear relaxation experiments under different compression strains.

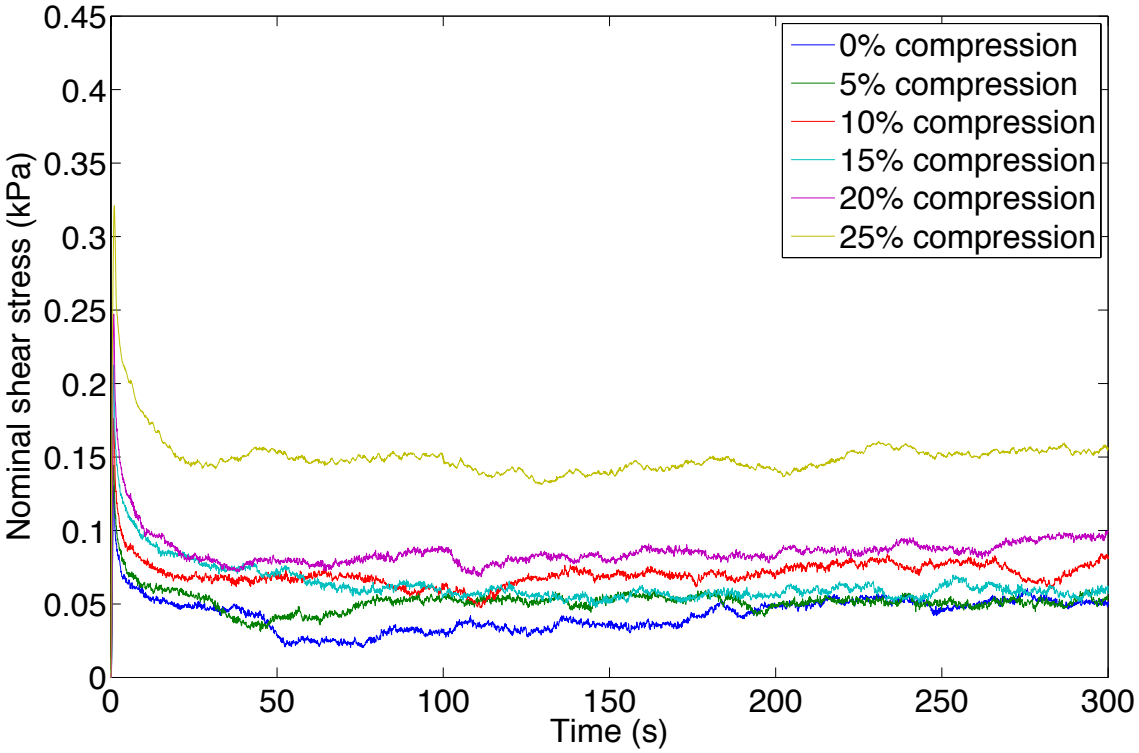


Figure 3.25: Nominal shear stress vs. time of one porcine brain sample tested in CSF. This graph depicts the results of the shear relaxation experiments under different compression strains.

Due to the fact that the influence of temperature plays an important role during the experiments, some trials were conducted at body temperature (37°C) to enable the comparison with the results at room temperature (22°C). To the best of the authors knowledge, only a few studies performed their tests at different temperatures [Peters et al., 1997] [Hrapko et al., 2008a]. Figures 3.26a and 3.26b show the results of the shear relaxation experiments at room temperature and body temperature.

Comparing these two figures it can be seen that the shear stresses at room temperature are higher than the one at body temperature, as described in Hrapko et al. [2008a]. Therefore one can assume that the tissue becomes softer with increasing temperature, as can be seen in Fig. 3.26b. One possible explanation for this effect could be that the brain tissue becomes softer and hence more elastic and less resilient with increasing temperature.

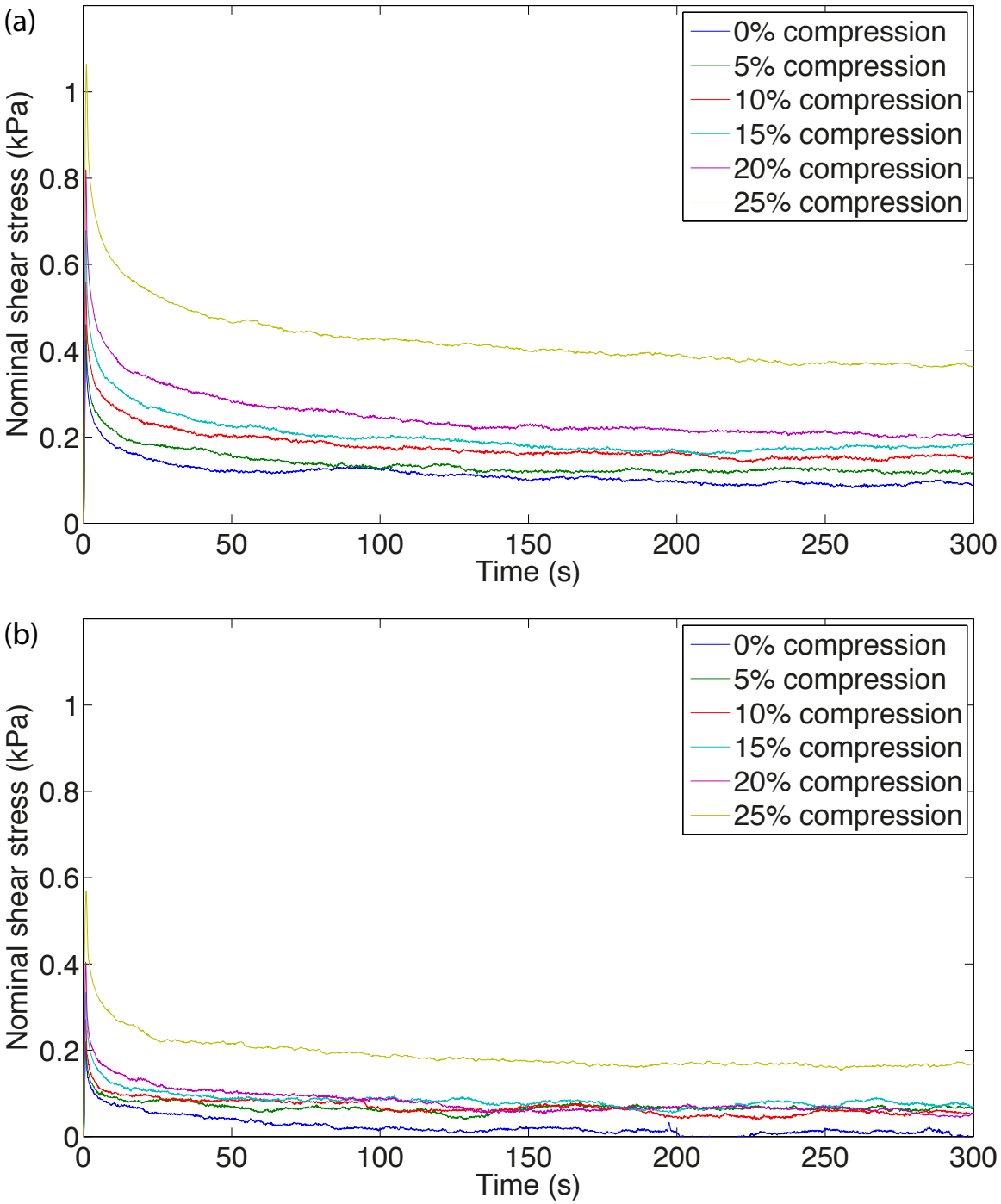


Figure 3.26: Shear relaxation experiments of one porcine brain sample. Graph in (a) depicts the results of the shear relaxation experiments at room temperature and graph in (b) exhibits the results at body temperature.

# 4 Discussion

Due to the fact that computational simulations are an important tool to estimate the stresses in brain tissues during traumatic brain injuries, brain development or hydrocephalus it is necessary to conduct more experiments, which provide the needed information for these simulations. Over the last several decades a lot of studies were conducted to determine the mechanical behavior of the brain tissue. Even though these studies contributed greatly to achieve a better understanding of the biomechanics of brain tissue, only few performed experiments under multiple loading modes, which are necessary as these tests allow to describe arbitrary loading conditions required for computational simulations [Budday et al., 2017a].

Therefore the current thesis provided new insights into the biomechanics of brain tissue by performing experiments under multiple loading modes. With the help of shear relaxation and cyclic simple shear experiments this master thesis confirmed the viscoelastic and nonlinear mechanical behavior of the brain, which coincides with other literature [Szotek et al., 2007] [Leondes, 2007] [Prevost et al., 2011a]. One main characteristic of the viscoelastic behavior was the hysteresis, which can for example be seen in the results of the simple shear experiments of a porcine sample in Fig. 3.1 and in the results of a human sample in Fig. 3.3. The hysteresis presented in the results of the simple shear experiments depicts an altered shaped, as a common hysteresis has sharp edges at the turning points. The reason for this alteration was, that due to the sinusoidal movement the strain rate decreased at the end of each shearing process, resulting in smooth edges, which can be seen in Section 4.1.

The viscoelatic behavior can also be seen in the shear relaxation experiments of Fig. 3.15. It can be described as the ratio between the maximum shear stress peak, at the beginning of each trial, and the shear stress equilibrium. The higher this ratio the more pronounced is the viscoelastic behavior. The nonlinear behavior of the brain tissue can also be seen in the nonlinear course of the simple shear experiments. For the results of the shear relaxation experiments with superimposed tension it can be seen that this augmentation of the shear stress only occurs in the range of 5% to a maximum of 20% tension strain.

One possible explanation for the decrease of the shear stress at 25% tension strain, which can be seen in Fig. 3.23b, could be that tension injuries of the axons already occur at 18% tension strain, as described in Bain and Meaney [2000]. In due consideration of the fact that tension injuries of axons occur at 18% tension strain [Bain and Meaney, 2000], the low shear stresses at 25% tension strain could be the result of tissue damage, caused due to the high tension strains.

Section 3 also displayed the increase of the shear stress with increasing compression strain and captured the stiffer response of the tissue with superimposed compression than with superimposed tension, as described in Budday et al. [2017a]. Further this master thesis described the regional dependencies of the brain tissue. Due to the small size of the specimens, it was possible to ensure that all prepared samples only consisted of one tissue type. As shown in Section 3 it can be seen that under slow loading rates gray matter tissue, such as the cortex and basal ganglia were stiffer than white matter tissue, corona radiata and corpus callosum. But under fast loading rates the opposite behavior occurs, and the corona radiate seems to be the stiffest region.

It can also be seen that for all experiments the corpus callosum was the softest region, which coincides with other studies [Budday et al., 2017a]. Due to the fact that some studies described the brain tissue to be nearly isotropic [Budday et al., 2017a] [Nicolle et al., 2004], all experiments conducted in this thesis were performed in one direction.

The results of the shear relaxation experiments under superimposed tension exhibited comparatively low shear stresses. One potential explanation for this could be that the sample was already saturated with PBS, due to the long duration of the experiment and the fact that the specimen was covered in it. Even though this condition, where the specimen is covered in PBS, is not the best solution to prevent dehydration, it still provides better insight in the biomechanics of the brain than the results of Fig. 3.23b, where the specimen was only humidified with PBS and therefore started to dry out, during the experiment. Due to the long duration of the experiments the humidified specimen started to dry out and the tissue became stiffer, which resulted in an increase of the shear stress. A better solution to prevent the specimen on the one hand from saturation and on the other hand from dehydration, could be with the help of steam. The steam would be generated by an electric kettle, which will then be inserted in the chamber through a pipe [Jin et al., 2013]. This steam would heat and humidify the air in the chamber and might prevent the specimen from saturation and dehydration [Jin et al., 2013].

Therefore it is necessary to cover the specimen with PBS, otherwise the mechanical properties would change, which would eventually lead to false assumptions. Due to the fact that the humidified specimen starts to dry out it becomes stiffer and one could assume that the shear stress with superimposed tension were higher than with superimposed compression, which can for example be seen in the comparison of Figs. 3.13 and 3.23b. The results of the shear relaxation experiments of only humidified specimens could also lead to false interpretations of the viscoelastic behavior, as the tissue becomes stiffer and therefore the ratio between the maximum peak of the shear stress and the shear stress equilibrium decreases, which might lead to the assumption that the viscoelastic behavior is less distinctive.

Due to the fact that some studies described the brain parenchyma as a fluid saturated porous material, consolidation theory has also be applied to brain biomechanics [Franceschini et al., 2006]. The average consolidation ratio is described as $U$ vs. time. As demonstrated by Franceschini et al. [2006], brain tissue not only behaves like a viscoelastic and nonlinear material but also like a fluid saturated porous material.

## 4.1 Limitations

One of the main problems during this master thesis was the preparation of the appropriate specimens. It was essential that all samples had the same dimensions, because otherwise a comparison between the different trials and the different brain regions would not be meaningful and might lead to false assumptions. Therefore it was necessary to cut cube shaped specimens with a side-length of 5 mm from each brain region. Due to the very soft tissue of the brain this preparation had to be done as fast as possible, to reduce tissue deformation, which would lead to a deformation of the specimen under its own weight.

Another problem was that due to the long duration of the experiment the tissue started to dehydrate, which resulted in an alteration of the mechanical properties. Therefore it was necessary to cover the specimen in PBS. But this led to the next problem. The tissue became saturated with water due to the length of each test, which probably resulted in the low strain rates during the tension tests, as they proceeded at the end of each trial. Therefore it is necessary to develop a testing procedure, which not only prevents the specimen from dehydration but also from saturation.

# 5 Conclusion

In this master thesis the nonlinear and viscoelastic properties of the brain tissue were confirmed, with the help of cyclic simple shear and shear relaxation experiments. These experiments were performed with superimposed compression and tension loadings, to achieve results under multiple loading modes. Further this master thesis described the regional dependency of the brain tissue under different loading conditions. According to the results shown in this thesis it could be seen that the cortex tends to be the stiffest region under low strain rates and it also depicts that the corpus callosum was the softest region under low and fast strain rates. The relaxation experiments demonstrated that under fast loading conditions the corona radiata became the stiffest region, which agrees well with previous studies [Budday et al., 2017b] [Jin et al., 2013]. These experiments additionally demonstrated the viscoelastic behavior of the brain tissue. It is described described as the ratio between the maximum shear stress peak and the, at the beginning of each trial, and the shear stress equilibrium. The higher this ratio the more pronounced is the viscoelastic behavior. According to Figs. 3.20 to 3.22 it can be seen that the ratio between the initial shear stress peak and the shear stress at the equilibrium seems to be the highest for the corona radiata.

By reason of the fact that the brain tissue not only consists of gray and white tissue, but also blood vessels and cerebrospinal fluid, it is necessary to consider the brain as a fluid saturated porous material, as described in Franceschini et al. [2006]. That is the reason why this thesis included a literature research on how the poroelastic properties of the brain tissue could be tested.

In the results of this thesis it could also be seen that due to the long duration of the experiments the humidified specimen started to dry out. Therefore it was necessary to cover the sample in liquid to prevent dehydration, which would lead to an alteration of the mechanical properties and finally to false assumptions.

# 6 Future Work

The main targets for future work should be to develop a testing device, which is capable to perform oedometric tests, to capture the poroelastic tissue properties. Such a device would contribute greatly to a better understanding of the biomechanics of brain tissue, as to the best of the authors knowledge only one paper so far conducted such tests on brain tissue [Franceschini et al., 2006]. This device is necessary to describe the poroelastic properties behavior of brain tissue.

Due to the limited availability of human brain samples, future studies should direct one's attention on the receiving of human brain specimens, as they would lead to more significant results than the one from porcine or bovine samples.

For future studies it might also be important to develop a testing procedure, which on the one hand prevents the specimen from dehydration and on the other hand from saturation. One possible solution could be the use of steam, which not only humidifies but also heats the air. This testing environment could lead to better results under superimposed tension, as the specimen is not covered in PBS and therefor not saturated with liquid.

Due to the fact that only a few studies performed experiments under multiple loading modes on the same specimen, which are necessary to describe arbitrary loading conditions, following studies should focus on performing such experiments. Such experiments are necessary to perform computational simulations, as they are needed to describe injuries such as traumatic brain injury or shaken baby syndrome.

# Statutory Declaration

I declare that I have authored this Thesis independently, that I have not used other than the declared sources/resources, and that I have explicitly marked all material, which has been quoted by the relevant reference.

| | |
|---|---|
| date | signature |

# Bibliography

AC Bain and DF Meaney. Tissue-level thresholds for axonal damage in an experimental model of central nervous system white matter injury. *Journal of biomechanical engineering*, 122(6):615–622, 2000.

LE Bilston, Z Liu, and N Phan-Thien. Linear viscoelastic properties of bovine brain tissue in shear. *Biorheology*, 34(6):377–385, 1997.

LE Bilston, Z Liu, and N Phan-Thien. Large strain behaviour of brain tissue in shear: some experimental data and differential constitutive model. *Biorheology*, 38(4):335–345, 2001.

MA Biot. General theory of three-dimensional consolidation. *Journal of applied physics*, 12(2):155–164, 1941.

S Budday, G Sommer, C Birkl, C Langkammer, J Haybaeck, J Kohnert, M Bauer, F Paulsen, P Steinmann, E Kuhl, et al. Mechanical characterization of human brain tissue. *Acta biomaterialia*, 48:319–340, 2017a.

S Budday, G Sommer, J Haybaeck, P Steinmann, GA Holzapfel, and E Kuhl. Rheological characterization of human brain tissue. *Acta Biomaterialia*, 2017b.

S Cheng and LE Bilston. Unconfined compression of white matter. *Journal of biomechanics*, 40(1):117–124, 2007.

KK Darvish and JR Crandall. Nonlinear viscoelastic effects in oscillatory shear deformation of brain tissue. *Medical engineering & physics*, 23(9):633–645, 2001.

R de Rooij and E Kuhl. Constitutive modeling of brain tissue: current perspectives. *Applied Mechanics Reviews*, 68(1):010801, 2016.

M Destrade, MD Gilchrist, JG Murphy, B Rashid, and G Saccomandi. Extreme softness of brain matter in simple shear. *International Journal of Non-Linear Mechanics*, 75:54–58, 2015.

BS Elkin, A Ilankovan, and B Morrison. Age-dependent regional mechanical properties of the rat hippocampus and cortex. *Journal of biomechanical engineering*, 132(1):011010, 2010.

GT Fallenstein, VD Hulce, and JW Melvin. Dynamic mechanical properties of human brain tissue. *Journal of Biomechanics*, 2(3):217–226, 1969.

H Ferner. *Anatomie des Nervensystems und der Sinnesorgane des Menschen*. Reinhardt, 1973.

G Franceschini, D Bigoni, P Regitnig, and GA Holzapfel. Brain tissue deforms similarly to filled elastomers and follows consolidation theory. *Journal of the Mechanics and Physics of Solids*, 54(12):2592–2620, 2006.

A Gefen, N Gefen, Q Zhu, R Raghupathi, and SS Margulies. Age-dependent changes in material properties of the brain and braincase of the rat. *Journal of neurotrauma*, 20(11): 1163–1177, 2003.

A Goriely, MGD Geers, GA Holzapfel, J Jayamohan, A Jérusalem, S Sivaloganathan, W Squier, JAW van Dommelen, S Waters, and E Kuhl. Mechanics of the brain: perspectives, challenges, and opportunities. *Biomechanics and modeling in mechanobiology*, 14 (5):931–965, 2015.

MW Greve and BJ Zink. Pathophysiology of traumatic brain injury. *Mount Sinai Journal of Medicine: A Journal of Translational and Personalized Medicine*, 76(2):97–104, 2009.

M Hrapko, JAW Van Dommelen, GWM Peters, and JSHM Wismans. The mechanical behaviour of brain tissue: large strain response and constitutive modelling. *Biorheology*, 43(5):623–636, 2006.

M Hrapko, JA Van Dommelen, GW Peters, and JS Wismans. The influence of test conditions on characterization of the mechanical properties of brain tissue. *Journal of Biomechanical Engineering*, 130(3):031003, 2008a.

M Hrapko, JAW Van Dommelen, GWM Peters, and JSHM Wismans. Characterisation of the mechanical behaviour of brain tissue in compression and shear. *Biorheology*, 45(6): 663–676, 2008b.

B Jennett. Epidemiology of head injury. *Journal of neurology, neurosurgery, and psychiatry*, 60(4):362, 1996.

X Jin, F Zhu, H Mao, M Shen, and KH Yang. A comprehensive experimental study on material properties of human brain tissue. *Journal of biomechanics*, 46(16):2795–2801, 2013.

M Kaczmarek, RP Subramaniam, and SR Neff. The hydromechanics of hydrocephalus: steady-state solutions for cylindrical geometry. *Bulletin of mathematical biology*, 59(2): 295–323, 1997.

W Kahle and M Frotscher. *Taschenatlas der Anatomie: Nervensystem und Sinnesorgane*. Thieme, 1991.

KM Labus and CM Puttlitz. Viscoelasticity of brain corpus callosum in biaxial tension. *Journal of the Mechanics and Physics of Solids*, 96:591–604, 2016.

K Laksari, M Shafieian, and K Darvish. Constitutive model for brain tissue under finite compression. *Journal of biomechanics*, 45(4):642–646, 2012.

JA Langlois, W Rutland-Brown, and KE Thomas. Traumatic brain injury in the united states; emergency department visits, hospitalizations, and deaths. 2006a.

JA Langlois, W Rutland-Brown, and MM Wald. The epidemiology and impact of traumatic brain injury: a brief overview. *The Journal of head trauma rehabilitation*, 21(5):375–378, 2006b.

CT Leondes. *Biomechanical systems technology*, volume 4. World Scientific, 2007.

CW MacMinn, ER Dufresne, and JS Wettlaufer. Large deformations of a soft porous material. *Physical Review Applied*, 5(4):044020, 2016.

SS Margulies and MT Prange. Regional, directional, and age-dependent properties of the brain undergoing large deformation. *J Biomech Eng*, 124:244–252, 2002.

JB Martinez, VOA Oloyede, and ND Broom. Biomechanics of load-bearing of the intervertebral disc: an experimental and finite element model. *Medical engineering & physics*, 19(2):145–156, 1997.

KF Masuhr, F Masuhr, and M Neumann. *Duale Reihe Neurologie*. Georg Thieme Verlag, 2013.

J Medige. Shear properties of human brain tissue. *Journal of biomechanical engineering*, 119:423, 1997.

K Miller and K Chinzei. Constitutive modelling of brain tissue: experiment and theory. *Journal of biomechanics*, 30(11):1115–1121, 1997.

K Miller and K Chinzei. Mechanical properties of brain tissue in tension. *Journal of biomechanics*, 35(4):483–490, 2002.

T Morris. Traumatic brain injury. In *Handbook of medical neuropsychology*, pages 17–32. Springer, 2010.

M Mumenthaler and H Mattle. *Kurzlehrbuch Neurologie, 1*. Thieme, 2006.

S Nicolle, M Lounis, and R Willinger. Shear properties of brain tissue over a frequency range relevant for automotive impact situations: new experimental results. *Stapp Car Crash Journal*, 48:239, 2004.

A Oloyede and ND Broom. Is classical consolidation theory applicable to articular cartilage deformation? *Clinical Biomechanics*, 6(4):206–212, 1991.

GWM Peters, JH Meulman, and AAHJ Sauren. The applicability of the time/temperature superposition principle to brain tissue. *Biorheology*, 34(2):127–138, 1997.

K Pogoda, L Chin, PC Georges, FRJ Byfield, Rt Bucki, R Kim, M Weaver, RG Wells, C Marcinkiewicz, and PA Janmey. Compression stiffening of brain and its effect on mechanosensing by glioma cells. *New journal of physics*, 16(7):075002, 2014.

TP Prevost, A Balakrishnan, S Suresh, and S Socrate. Biomechanics of brain tissue. *Acta Biomaterialia*, 7(1):83–95, 2011a.

TP Prevost, G Jin, MA De Moya, HB Alam, S Suresh, and S Socrate. Dynamic mechanical response of brain tissue in indentation in vivo, in situ and in vitro. *Acta biomaterialia*, 7 (12):4090–4101, 2011b.

B Rashid, M Destrade, and MD Gilchrist. Mechanical characterization of brain tissue in simple shear at dynamic strain rates. *Journal of the mechanical behavior of biomedical materials*, 28:71–85, 2013.

B Rashid, M Destrade, and MD Gilchrist. Mechanical characterization of brain tissue in tension at dynamic strain rates. *Journal of the mechanical behavior of biomedical materials*, 33:43–54, 2014.

S Sivaloganathan, M Stastna, G Tenti, and JM Drake. Biomechanics of the brain: a theoretical and numerical study of biot's equations of consolidation theory with deformation-dependent permeability. *International Journal of Non-Linear Mechanics*, 40(9):1149–1159, 2005.

M Stastna, G Tenti, S Sivaloganathan, and JM Drake. Brain biomechanics: consolidation theory of hydrocephalus. variable permeability and transient effects. *Canadian Applied Mathematics Quarterly*, 7:111–124, 1999.

S Szotek, M Kobielarz, and K Maksymowicz. Mechanical response of brain to mechanical stimuli-animal model investigation. *Neurologia i neurochirurgia polska*, 41(6):525, 2007.

Y Tada, T Nagashima, and M Takada. Biomechanics of brain tissue: Simulation of cerebrospinal fluid flow. *JSME international journal. Ser. A, Mechanics and material engineering*, 37(2):188–194, 1994.

A TAMURA, S HAYASHI, I WATANABE, K NAGAYAMA, and T MATSUMOTO. Mechanical characterization of brain tissue in high-rate compression. *Journal of biomechanical science and engineering*, 2(3):115–126, 2007.

A Tamura, S Hayashi, K Nagayama, and T Matsumoto. Mechanical characterization of brain tissue in high-rate extension. *Journal of Biomechanical Science and Engineering*, 3(2):263–274, 2008.

K Terzaghi. *Theory of consolidation*. Wiley Online Library, 1943.

JAW Van Dommelen, TPJ Van der Sande, M Hrapko, and GWM Peters. Mechanical properties of brain tissue by indentation: interregional variation. *Journal of the mechanical behavior of biomedical materials*, 3(2):158–166, 2010.

AJ Waldeyer. *Waldeyer–anatomie des menschen*. walter de Gruyter, 2009.

J Weickenmeier, R de Rooij, S Budday, P Steinmann, TC Ovaert, and E Kuhl. Brain stiffness increases with myelin content. *Acta biomaterialia*, 42:265–272, 2016.

RZ Zhan and JV Nadler. Enhanced tonic gaba current in normotopic and hilar ectopic dentate granule cells after pilocarpine-induced status epilepticus. *Journal of neurophysiology*, 102(2):670–681, 2009.